Annu. Rev. Astron. Astrophys. 2002. 40:439–86
doi: 10.1146/annurev.astro.40.060401.093849

SHAPES AND SHAPING OF PLANETARY NEBULAE

Bruce Balick
Department of Astronomy, University of Washington, Seattle, Washington 98195-1580; email: balick@astro.washington.edu

Adam Frank
Department of Physics and Astronomy, University of Rochester, Rochester, New York 14627-0171; email: afrank@pas.rochester.edu

Key Words stellar evolution, mass loss, protoplanetary nebulae, hydrodynamics, magnetohydrodynamics

■ **Abstract** We review the state of observational and theoretical studies of the shaping of planetary nebulae (PNe) and protoplanetary nebulae (pPNe). In the past decade, high-resolution studies of PNe have revealed a bewildering array of morphologies with elaborate symmetries. Recent imaging studies of pPNe exhibit an even richer array of shapes. The variety of shapes, sometimes multiaxial symmetries, carefully arranged systems of low-ionization knots and jets, and the often Hubble-flow kinematics of PNe and pPNe indicate that there remains much to understand about the last stages of stellar evolution. In many cases, the basic symmetries and shapes of these objects develop on extremely short timescales, seemingly at the end of AGB evolution when the mode of mass loss abruptly and radically changes. No single explanation fits all of the observations. The shaping process may be related to external torques of a close or merging binary companion or the emergence of magnetic fields embedded in dense outflowing stellar winds. We suspect that a number of shaping processes may operate with different strengths and at different stages of the evolution of any individual object.

INTRODUCTION

PN Morphologies: The Smirk of the Cheshire Cat

Perhaps the first and youngest of the many "standard models" in astronomy to fall victim to the penetrating spatial resolution and dynamic range of the Hubble Space Telescope (HST) was that for planetary nebulae (PNe). Historically, in 1993, Frank et al. confidently claimed that the morphologies of nearly all PNe could be understood as the evolving hydrodynamic interaction between fast winds from a central star and the nozzle formed by a dense torus of material presumably ejected earlier in the life of the central star. In 1994, the now-famous HST image of the Cat's Eye Nebula (Harrington & Borkowski 1994) mocked Frank et al.'s simple paradigm in several ways. First, no signs of dense tori were seen in close association

with either member of an odd pair of orthogonal ellipsoidal features in the nebular core. Second, the HST image showed an incredible array of meticulously organized knotty or jet-like features that extant hydro models simply cannot explain with any credible set of presumed initial and boundary conditions. Insofar as our comprehension of the shapes of PNe is concerned, the HST image of NGC 6543 is redolent of the frustrating ambiguity of the Cheshire Cat.

HST images of other PNe with very different but equally spectacular structures and symmetries followed quickly. Each new image was greeted with a combination of aesthetic delight and interpretive apprehension, if not terror, by nebular dynamicists. Taken together, and divided into morphological classes, the complex symmetries of PNe raise embarrassing issues for our understanding of stellar evolution as well as difficult questions about the physics of gas dynamical processes. The underlying issue raised by modern images of PNe is how gasping, dying stars with huge, fluffy, marginally bound atmospheres can produce such complex but highly organized outflows. This paper 1. reviews the morphologies and their first derivative, the kinematics of both planetary nebulae and their progenitors, protoplanetary nebulae (pPNe); 2. summarizes the astronomical and physical challenges revealed by the data; and 3. probes the physical shaping mechanisms of PNe.

Studies of nebular dynamics in PNe are probably extensible to other more elusive types of outflows. The resemblance of some PNe to H-H objects, YSOs, η Car, some axisymmetric supernovae, and bipolar AGNS is striking. For example, compare the pairs of rings near SN1987A (e.g., Burrows et al. 1995) with the similar rings in MyCn18 (Sahai et al. 1999b) and He2-104 (Corradi et al. 2001) that are inscribed in their bipolar lobes. Obvious counterparts to the "homunculus" of η Car (Morse et al. 1998), a rapidly expanding bilobed LBV nebula, are Menzel 3 (Redman et al. 2000) and Hubble 5 (Riera et al. 2000). He2-90 (Sahai & Nyman 2000, Guerrero et al. 2001) is a dead ringer for an H-H object, other than it has no connection whatsoever to a star-forming region. Therefore some of the mechanisms that shape PNe may have broad application in related objects such as YSOs in which extinction or distance often occlude the dynamically important regions.

PNe research is entering another renaissance. This is a time of intellectual puzzlement, debate, and play in which the imaginations of observers and theoreticians are crossing disciplinary boundaries in order to explain the morphologies and kinematics of PNe and pPNe. PNe are the testing grounds for many of these ideas thanks to their brightness, the full range of their shapes, the paucity of local extinction, and their large numbers. The expanding constellation of interpretive ideas that has emerged to explain PN morphologies are ready to be organized and reviewed.

The Historical Setting

The modern field of PNe mass ejection started when Deutsch (1956) found displaced absorption lines in the spectrum of α Her and concluded that late-type AGB

stars and supergiants were shedding their outer layers. Shklovskii (1956a,b) and Abell & Goldreich (1966) showed how luminous AGBs might eject their envelopes via structural instabilities. Within a decade the idea that subsurface shell flashes and/or surface pulsations could drive loosely bound matter from AGB stars had gained popularity, though the effectiveness of each mechanism remained unclear.

It is now well established that AGB and post-AGB stars lose mass at rates as high as 10^{-5} $M_\odot$ yr^{-1} or more at super-escape velocities of about 10 km s^{-1}. The general idea is that during the AGB phase IR photons accelerate dust particles that then drag the gas with them to form a nebula. Acoustic waves and surface pulsations might provide an additional boost (Pijpers & Hearn 1989; Pijpers & Habing 1989). Mass loss mechanisms from cool giant stars have been reviewed thoroughly by Willson (2000).

Until 1978 it was believed that mass loss ceased at this point and the ejected envelope expanded isotopically. A paradigm shift occurred with the opening of the ultraviolet window. Kwok et al. (1978), Cerruti-Sola & Perinotto (1989), Patriarchi & Perinotto (1991), and others found that as the star evolves from AGB to PN nucleus, its mass loss rate decreases precipitously (10^{-8} $M_\odot$ yr^{-1}) but does not cease. At the same time, the speed of the winds, V_w, rises almost reciprocally, from about 10 to 10^3 km s^{-1}. The material ejected earlier becomes ionized once the temperature at the exposed surface of the central "nucleus" exceeds 25,000 K. Eventually, hard uv photons (10–50 eV) couple strongly to blanketed lines of multiply ionized metals (Lamers & Cassinelli 1999). Multiple scattering of the uv photons in the dense acceleration zone could enhance the radiation pressure and drive the wind with a momentum flux $\tau_{scat} \cdot L_*/c$, where $\tau_{scat} \leq 10$ is the scattering opacity.

In general, all winds driven by these mechanisms are inherently isotropic; however, the fruits of their labors, pPNe and PNe, conspicuously display a variety of symmetries. The present controversy is how axisymmetric and more complex types of pPNe and PNe form and evolve. Astronomically, how do highly evolved stars in isolated environments collimate their outflows and orchestrate the grand design of the nebula? Physically, what is the nature of the shaping process(es)?

Wind-Shaping 101

Here we describe the basic concept behind the now-challenged standard model of PN morphologies (a fuller description appears in "Variations on a Theme: Theoretical Models"). Kwok et al. (1978) introduced the interacting stellar wind (ISW) concept into the field of PNe. Fast stellar winds quickly overtake the slower, denser material ejected as or just after the AGB phase and interact hydrodynamically with it. In steady state, fast winds do not reach the "slow winds" directly. Most of the kinetic energy in fast winds is first converted to thermal energy at a generally radiationless shock where the ram pressure of the diluted wind matches the pressure in the world upstream. If the fast wind speed exceeds 150 km s^{-1}, then a "hot bubble" (10^{7-8} K) with a large adiabatic sound speed forms just ahead of this shock. Its

high internal pressure pushes the bubble supersonically into the older and denser gas upstream. Hence, the expanding bubble displaces and sweeps the slow wind into a thin, compressed, efficiently cooling dense rim at its leading edge.

Consequently, if we assume isotropy of the old slow and young fast winds, then all PNe should consist of a hot, nearly invisible central cavity separated from a smooth mantle of slow winds by a bright rim of plowed-up gas. The potential relevance of ISW models is nicely confirmed by most round and mildly elliptical PNe, such as IC 3568 and NGC 3132 (Figure 1). Frank et al. (1990) demonstrated detailed agreement between predictions of ISW models and the observed density distribution, or shells, of round PNe. (Hereafter we avoid the use of the term "shell" that has become extremely ambiguous over the years.)

Bipolar PNe—those with two lobes on opposite sides of the nuclear region—form a greater challenge to explain. Calvet & Peimbert (1983) were the first to suggest that a dense circumstellar torus can deflect the winds toward a polar axis and form a pair of expanding bubbles. Kahn & West (1985) used analytical calculations to demonstrate the plausibility of the mechanism. Balick (1987), Balick et al. (1987), and others observationally confirmed that dense equatorial disks gird the bright rims of nearly all axisymmetric PNe. Analytic and numerical studies of fast winds by disks and tori by Icke (1988), Icke et al. (1989, 1992), Soker & Livio (1989), Frank (1994), Mellema (1994, 1995), and Mellema & Frank (1995) followed shortly. Their calculations became known as generalized ISW (GISW) models discussed in detail in "Variations on a Theme: Theoretical Models."

The origin of the putative collimating disk or torus remains a matter of conjecture to this day. Historically, Morris (1981, 1987), Soker & Livio (1989), and many others suggested that the disks could be the remnants of binary mergers and tidal interactions. As observations have improved, PN morphologies with far too much high-order structure (e.g., multiple pairs of lobes each with their own axes of symmetry, and jets of very thin cross section) have clearly demonstrated that GISW models are, by themselves, inadequate. Meanwhile, additional paradigms such as magnetic collimation have emerged as well. The pursuit of the paradigms and the data that constrain them are the subject of this review.

Scope of this Review

Samuel Clemens once quipped that horse races are less interesting than the people who bet on them. The same is true for PNe research. In "Classical PNe" and "ProtoPNe" we'll examine the horses, PNe and pPNe, and organize their properties. In "Observational Results and Questions: Summary" we develop a list of issues that need insight and understanding. In "Variations on a Theme: Theoretical Models" below we shall look at the bettors: the mechanisms proposed to account for the observed morphologies and kinematics of PNe and pPNe. A brief summary and assessment of the field is given in "Conclusions and Future Directions." Regretfully, we cannot consider the growing body of research regarding the central

stars, chemical abundances, luminosities, masses, distances, radiative wind-driving mechanisms, ionization structures, numbers, or galactic distribution of PNe.

CLASSICAL PNe

Organizing PNe: Morphological Types

Like the taxonomy of moths, nebular classification is important as it can uncover recurrent patterns and themes that reveal common outcomes of processes shaping PNe and other nebulae. A useful system must be based on clear class definitions, be easy to apply, and incorporate the vast majority of nebulae. Here we describe two complementary systems, both of which are widely used.

The most common description of global morphology, originally assembled from ideas in the literature and evaluated by Balick (1987), is based on the outline of the spatially resolved nebula. The four basic nebular types are Round (R, prototype IC 3568), Elliptical (E, NGC 3132 and 6826), Bipolar (Bp, a pair of lobes), and irregular (relatively rare). [See Figure 1 for images of prototypes.] The first three classes are not completely distinct: Mildly elliptical nebulae form the transition from R to E, and peanut-shaped objects divide the E and Bp classifications. It is very important to note the Galactic scale height of Bp PNe, 130 pc, is that of $\geq$1.5 $M_\odot$ stars, whereas E and R PNe have the same scale height of $\leq$1.1 $M_\odot$ stars (Zuckerman & Aller 1986, Corradi & Schwarz 1995). Therefore, Bp nebulae almost certainly evolve from higher-mass progenitors than other types.

In this paper we subdivide Bp into "butterfly," in which the waist is pinched into the center, and "bilobed" PNe, in which a pair of larger outer lobes connects to a central and generally smaller R or E nebula. M2–9 (Doyle et al. 2000) and He2-104 (Corradi et al. 2001) are examples of the former and NGC 6886 and 7026 are characteristic of the latter. [See Figure 1 and Corradi & Schwarz (1995), Balick (2000) and López (2000) for image galleries of these and other bilobed and butterfly PNe.] The bipolar class has recently been generalized to quadrupolar and multipolar (Manchado et al. 1996, Guerrero & Manchado 1998, Muthu & Anandarao 2001).

GISW models predict that bilobed PNe will form as the interior hot bubble punctures the outer edge of the confining mantle on the symmetry axis (Balick 1987, Icke et al. 1989). The lobes grow rapidly at first as the escaping hot gas plows outwards into sparse gas outside the mantle and cools adiabatically. The growth of the lobes is decelerated as ambient material of relatively low specific momentum is accreted. This compressed material will cool and may partially recombine in time.

The structure and kinematic patterns of butterfly PNe are much more complicated and diverse than for bilobed PNe. We consider the properties of butterfly PNe later in this section. For now we note that several of them have luminous and relatively cool central stars sometimes showing spectral features of symbiotics or

Miras. Thus, they may be bone fide PNe based on morphological selection criteria; nonetheless, their central stars will not reside in the H-R diagram on the evolutionary tracks where most other PN nuclei are found, and the history of their evolution may not be consonant with true PNe.

All morphological classes are blurred by projection effects (Frank et al. 1993). For example, ellipticals and bipolars degenerate into round PNe when we view the nebulae along their symmetry axes. In addition, the morphological classes can depend somewhat on the emission line used for making an image. It is not unusual for images obtained in [NII] and [OI] lines to appear edge-brightened, whereas [OIII] and Hα emission seems to arise in the nebular interior. Any taxonomic system that is based on outlines is best defined from the former, low-ionization images in which the nebular edges are generally exaggerated.

A second classification scheme favored by Manchado, Stanghellini, Corradi, and others is based on the highest degree of overall symmetry of the nebular interior. The basic types are axisymmetric, reflection symmetric, point symmetric, and asymmetric. The first requires reflection symmetry around the major and minor axes, the second requires reflection symmetry about the minor axis only, the third requires symmetry only through the nebular center, and the final category has no symmetry about an axis or point. Most PNe are very nearly axisymmetric. Point-symmetric nebulae tend to be S-shaped, corkscrew-like, or multipolar (showing more than one axis of symmetry). Reflection-symmetric PNe are rare; M2–9 is an example since its lobe edges are brighter on one side than the other.

Some PNe have striking symmetries that combine or transcend standard taxonomical schemes above. The crossed ellipses of the Cat's Eye Nebula were already mentioned. Hu 2–1 is the PN equivalent of a Russian doll, with nested nebulae of highly elliptical outlines at various position angles (Miranda et al. 2001b). Sahai & Trauger (1998) published images of several very compact, low-ionization (young) PNe that have striking multi-axis symmetries, some of which look like textbook hydrogen wave functions! Any process that forms such high-order symmetries requires a high degree of global coordination or internal communication. We note also that in some cases certain emission characteristics may single out morphological types as in H_2 emission for bipolar nebula (Kastner et al. 1994, 1996).

Knots and Jets

In addition to the global structures, so-called "fine structures," such as knots and jets, are found in about half of PNe (see review by Gonçalves et al. 2001). It is common for the knots and jets to appear primarily or exclusively in emission lines of low ionization, so Gonçalves et al. suggested the acronym "LIS" (low-ionization structures) for them. Many knots have directly associated tails that point radially outwards (O'Dell & Ball 1985, O'Dell & Handron 1996, Balick et al. 1998). Such a morphology indicates the tails develop when winds from the central star sweep into gas ablating or evaporating from dense neutral knots.

A special subclass of LIS are FLIERs, or Fast Low-Ionization Emission Regions, in which symmetric pairs of low-ionization knots exhibit distinctly opposite,

supersonic Doppler shifts ($\geq$20 km s^{-1}). These high Doppler shifts imply that FLIERs have a smaller kinematic age than the gas that surrounds them. They appear to be enriched in nitrogen/oxygen (N/O) (Balick et al. 1994), so they may have been ejected directly from the central star after the slow wind ejection ended. But this picture is incomplete. For example, ejected material should produce bow shocks whose heads point outwards; however, the reverse is found (Balick et al. 1998). [See López (2000) and "Variations on a Theme: Theoretical Models" below for a more extensive summary of FLIERs.]

The word "jets" is generally restricted to thin and often radial features with no visible sign of widening. (Jets and thin tails are functionally the same morphology.) Some jets have corkscrew shapes, called Bipolar Episodic Rotating jeTs (BRETs) (López et al. 1993; see reviews by López 1997, 2000). Unlike H-H objects/jets, the base of nearly all visible jets in PNe is widely separated from their central star.

Knots in the Helix Nebula (appearing by the hundreds) have been studied intensively by O'Dell and collaborators in a series of papers. Knots like these, many with long radial tails, are also found in the Eskimo, the Dumbbell, Abell 30, and other PNe where their properties are fairly similar. These knots exhibit surface ionization that is strongest where the knots directly face the star. O'Dell concluded that the knots are being slowly photoevaporated, and that the evaporated gas is swept back by gentle outflowing winds. Meaburn et al. (1998) found the knots to be moving radially more slowly than the outflowing winds in which they are immersed. They assert that the knots are primarily eroded by the wind. However, O'Dell et al. (2000) show that the emission is extremely well modeled by simple photoionization alone. The aggregate gas dispersed from these knots may very well determine the large-scale morphology and line flux of some of their parent nebulae, such as the Helix, at least at the present time. It is extremely unclear how or why the knots form in such large numbers and highly organized patterns.

The kinematics of small features—usually LISs—show exciting but puzzling results. [See the excellent review and synthesis of the kinematics of LISs by Gonçalves et al. (2001).] We have already mentioned that FLIERs come in pairs with equal but opposite supersonic velocities. Extremely high speeds in remote knots along the symmetry axis of some butterfly PNe—up to 630 km s^{-1} for MyCn18 (O'Connor et al. 2000), 500 km s^{-1} for Menzel 3 (Redman et al. 2000), 350 km s^{-1} for He2–111 (Meaburn & Walsh 1989), 164 km s^{-1} for M2–9 (Schwarz et al. 1997), and 300 km s^{-1} for M1–16 (Corradi & Schwarz 1993b)—are more the rule than the exception. These speeds pose huge challenges for GISW models since the transfer of momentum from stellar winds ($V_w \approx 10^3$ km s^{-1}) to nearby dense gas is not very efficient.

Halos

A halo often surrounds the core of a far brighter round or elliptical PN core at the halo's center. Halos are almost exclusively round in shape, very faint in surface brightness, smooth or slightly mottled, and limb-brightened (an exception is the outermost halo of the Cat's Eye Nebula). Most halos seem to be spherical bubbles

seen in projection. Some of the deepest images are by Balick et al. (1992) and Hajian et al. (1997). The properties of halos are summarized by Terzian & Hajian (2000).

Frank et al. (1990) used hydrodynamic modeling to show that the density distributions of single ring-like halos are consistent with an earlier and highly evolved episode of mass ejection expanding into an isotropic medium. The most complete observational investigations of individual halos are by Bryce et al. (1992a,b) and Bryce et al. (1994). Their kinematical observations do not always confirm this picture.

Recent observations of halos in both PNe and pPNe have revealed a second type of halo morphology: more or less evenly spaced concentric rings or arcs (e.g., Sahai et al. 1998, Balick et al. 2001, Hrivnak et al. 2001) that lie outside of but in close contact with their brighter cores. Again, these nested features are interpreted to be the edges of concentric bubbles or bubbles segments seen in projection. These are found in pPNe and PNe of sundry morphological types including bipolars.

For halos composed of concentric rings or arcs, the intra-bubble time scales are close to 1000 years. The repetition periods of surface pulsations are much shorter ($\leq$10 years), and core flash timescales are much longer ($\sim 10^5$ years). Simis et al. (2001) have found a hydrodynamic instability in dusty outflows with the appropriate 1000-year timescale. García-Segura et al. (2001) show that regularly spaced bubbles can be created by pressure waves associated with periodic reversals of the stellar magnetic field.

One implication of the both single and concentric halos surrounding much more structured inner PNe is that the mode of stellar mass loss changes abruptly from isotropic to something far more complex, dense, massive, and structured. Judging from the images, the mode change is abrupt and permanent. As we show later, the change is likely to occur near the end of the AGB phase of evolution as the PN phase commences.

Large-Scale Kinematics and Proper Motions

Speaking crudely, kinematics and proper motions trace the first derivative of the nebular structure. Hence kinematic studies bear directly on our understanding of nebular shaping processes. The primary technique of probing nebular kinematics has been Doppler shift mapping using an imaging Fabry-Perot interferometer or a multiple long-slit, high-dispersion (Echelle) spectrograph.

The most systematic studies of the kinematics of individual PNe are by Meaburn, Bryce, López, and other collaborators (since 1980); Miranda, Solf and several collaborators over the past 20 years; Balick et al. (1987) and Icke et al. (1989); Corradi and various collaborators (starting in 1993); Cuesta, Phillips, Mampaso and their collaborators (from 1993); Guerrero et al. (1998). Compilations of, and a search for, statistical trends in kinematic data from many PNe by Weinberger (1989) and Sabbadin (1984), Sabbadin et al. (1984), and Sabbadin et al. (1986) are still very useful.

In summary, R and E nebulae expand almost uniformly and homologously. Smooth mantles expand in such a way that velocity scales with distance. The bright rims on the inside edges of the mantles are generally expanding faster than the inner mantle, as expected where the bubble is overtaking and plowing up the material upstream from it. Gas motions reflect the symmetries of the structure with which they are associated. R and E PNe expand radially and tend (with minor exceptions) to grow faster along their projected symmetry axis than in their equatorial plane. This is as might be expected if they are to maintain their overall shapes as they evolve. Bilobed (as distinct from butterfly nebulae) follow the trend of ellipticals.

The kinematic patterns for butterfly PNe often reveal a more complex story. M1–16, Hubble 5, NGC 6537 (Corradi & Schwarz 1993a,b; Huggins et al. 2000) and He2–104, (Corradi et al. 2001) exhibit patterns of "Hubble Flows"; i.e., radial outflows whose speeds increase linearly with distance from the nucleus. Corradi et al. surmised that the expansion of three very distinct morphological components of He2-104 all have the same expansion age, suggesting that these three parts of the nebulae were formed in one event and then flung ballistically outward. In contrast, two butterfly nebulae exhibit fairly constant velocities with radial offset in their inner regions (e.g., M2–9, Solf 2000; He2–90, Guerrero et al. 2001). This kinematic pattern is much as expected for a constant, sustained outflow from the wind source, much as seen in most H-H systems. Why this kinematic signature is common in YSOs and rare in PNe is not clear.

Another method of charting the internal motions of PNe is to make a time series of images. The resulting movies provide dynamical information that nicely complements Doppler-velocity mapping. Multi-epoch images spanning two to five years with sufficient spatial resolution to monitor the changes in the structure of over a dozen PNe are being obtained by Hajian and his collaborators. Reed et al. (1999) found that NGC 6543 has expanded fairly uniformly (by a magnification factor of 1.00275) in three years. Schwarz et al. (1997) found a similar pattern in the outer regions of M2–9. Similar self-similar patterns have been found in some shocked pPNe such as OH231 ("ProtoPNe). Distances to these nebulae can be found using expansion parallax.

Nebular Momenta

All of the wind's momentum is transferred into the snowplowed gas in the rim of a model wind-blown bubble. Note, however, that only 20% of the wind's kinetic energy is deposited (Dyson & Williams 1980). It is therefore useful to compare the momenta of the nebula to that supplied by stellar radiation since the AGB phase to see if radiatively driven stellar winds are likely to be the driving mechanism behind PNe.

The cumulative momentum of a radiatively driven wind P_w is $(L_*/c)\Delta t$, where L_* is the luminosity of the star during its nebular expansion lifetime Δt. A low-mass star will sustain a luminosity of $\sim 10^3$ $L_\odot$ for about 10^4 year, providing a cumulative

wind momentum P_w of about $10^{37.5}$ g cm s^{-1}. By comparison, a typical round or elliptical PN consists of about $\sim$0.2 $M_\odot$ with an expansion velocity of 10 km s^{-1} ahead of the expanding hot bubble in its interior. The corresponding momentum of the nebula, P_{neb}, is 10^{39} g cm s^{-1}. Multiple scattering of photons at the base of the wind is believed to account for the momentum excess $P_{neb}/P_w \sim \tau_{scat} \sim 10$–20. Hence the nebular momentum agrees with expectations of ISW models.

Higher-mass central stars have higher luminosities and somewhat offsetting shorter evolution times, or about the same P_w as for their lower-mass counterparts. The masses of their bipolar nebulae (up to 1 $M_\odot$ in ionized and molecular gas) and outflow speeds (20–50 km s^{-1}) are several times larger than for round and elliptical PNe. Bujarrabal et al. (2001) find that the momentum budgets of Bp nebulae are in accord with the momentum yield from their luminosity-driven winds.

Extended X rays in PNe

The Chandra X-ray telescope was the first to map extended X rays in the elliptical PNe BD + 30°3639 (Kastner et al. 2000), NGC 7027 (Kastner et al. 2001) and NGC 6543 (Chu et al. 2001a,b), and more efforts are under way.

So far, X rays are closely associated with the innermost optically dark hot bubbles of these three nebulae. The observed X-ray emission temperatures are 10^6 K whereas ISW models predict temperatures as much as 100 times hotter. Mixing of hot gas with much cooler, denser gas across the contact discontinuity is ruled out because each region is observed to be chemically differentiated. Thus the observations suggest that additional physics, such as thermal conduction, must be added to ISW models to properly describe the growth of the interior structure of the hot, expanding bubble and its impact on the slower gas upstream.

PROTOPNe

Several pPNe had been identified prior to 1990, most all of them owing to their unusual IR or molecular properties. The best known of these are CRL 618, CRL 2688 (the Egg), IRC + 10216, HR 44179 (the Red Rectangle), and IRAS09371 + 1212 (Frosty Leo). These and a few others were legacies of opportunistic discoveries—some from observations of radio and IR molecular lines, and others from early IR surveys done during the 1970s and 1980s. These early pPNe were the tip of the iceberg; many more, most of them heavily obscured, were found starting in the 1980s as IR measurements improved. Today, hundreds of IR color-selected candidate objects and OH/IR stars have been identified, all of which can be loosely described as pPNe.

AGB and post-AGB stars are differentiated from each other and YSOs in two ways: van der Veen & Habing (1988) and van der Veen et al. (1989) showed how the IR colors of pPNe systematically distinguish them their state of evolution as the central star evolves from AGB to PN nucleus. In addition, Kwok (1993) and his collaborators showed that the IR spectral energy distributions (SEDs) of pPNe

undergo a qualitative change as the star enters the post-AGB phase of its evolution. Kwok attributes the changes of the SEDs to the ejection and detachment of a cool shell from the core as the star evolves from AGB to post-AGB states.

pPNe are just beginning their expansions, so they tend to be intrinsically small. pPNe lifetimes are short, so they tend to be rarer and, hence, located at larger distances than typical PNe. Most pPNe are (or have recently been) forming dust particles, which heavily obscure them. In spite of all of these difficulties, optical images of pPNe in dust-scattered starlight and IR images in thermal dust continua, along with emission-line images of extremely youthful PNe, show that pPNe are just as important to understanding mass outflow properties of AGB and post-AGB stars as are PNe, their much brighter, less obscured, and more mature siblings.

Morphology: Optical and IR Continuum Observations

The first systematic imaging survey of pPNe by Kwok et al. (1996) uncovered about a dozen resolved pPNe. They found that the morphologies of these pPNe had about the same distribution of morphological types as ordinary PNe and surmised that PNe originally obtain their underlying symmetries during the slow-wind phase of mass loss. This work, which was limited by a small sample size and poor spatial resolution, was prescient.

HST images have been obtained for several pPNe with post-AGB nuclei, and the results are as spectacular as they are unanticipated. These images, made in reflected starlight and emission lines arising in shocks, show striking bipolar and multipolar symmetries and in several cases, large multiple outer halos. Two such HST images appear at the bottom of Figure 1. Many more observations can be found in Kwok et al. (1998, 2000), Su et al. (1998), Hrivnak et al. (1999, 2001), Skinner et al. (1998), Ueta et al. (2000), Sahai et al. (1998, 1999a,c, 2000); Trammell & Goodrich (1996) and others.

Sahai & Trauger (1998) published a gallery of some of the most stunning of all HST imaging observations. Their targets are very young PNe that not surprisingly are small in size, low in overall ionization, and high in IR excess flux (Zhang & Kwok 1993). These criteria select objects in transition from pPNe to classical PNe in which the central star is just starting to ionize the gas. A few evolved low-ionization bipolars fell into their net; we ignore these here. The remaining objects show a panoply of morphologies, all of them exhibiting startlingly high-order symmetries—more so than mature PNe. Many have several axes of symmetry in different orientations. Names such as "starfish" (He2-47 and He2-339; see Figure 1) tell the story. Similar starfish morphologies have been found in outflows of various traditional pPNe (CRL 2688—Cox et al. 2000; CRL 618—Trammell 2000, Ueta et al. 2001; IRAS 16594-4656—Hrivnak et al. 1999; Roberts 22—Sahai et al. 1999c; and Frosty Leo—Sahai et al. 2000). Other young PNe such as He2–131 and He2–138, have serpentine inner boundaries that resemble atomic wave functions. For a recent compilation of observations of these young objects see Section 1 of Sahai (2000).

Although the many odd morphologies of pPNe and very young PNe are unexplained, several straightforward conclusions emerge: 1. as suggested by Sahai & Trauger, GISW models simply do not have the complexity necessary to account for the common high-order symmetries; 2. the winds that form these complex structures may not be isotropic; and 3. normal PNe only rarely show such high-order symmetries. The last conclusion suggests that fast winds, hot bubbles, and ionization fronts burnish or eradicate many structural details and, consequently, invite an unrealistically simplistic approach to constructing hydrodynamic models. Sahai & Trauger proposed that the multipolar lobes form as a flailing nozzle ejects occasional jets. Several authors have proposed that such complex symmetries mandate magnetohydrodynamic models ("Variations on a Theme: Theoretical Models").

Morphologies of pPNe with AGB Nuclei

Imaging studies specifically directed at stars in their AGB phase, though relatively few in number, show that mass loss is generally isotropic. IRC + 10216 is a spectacular example of a halo of a pPNe in its AGB phase that consists of multiple concentric dust shells—actually, more like arc segments with irregular spacings of 200–800 years (Mauron & Huggins 1999, 2000). Dust rings and asymmetries have been mapped with lower resolution in several other post-AGB stars: (AC Her—Jura et al. 2000, HD 56126—Jura et al. 2000) and other papers cited therein. Jura & Kahane (1999) discuss orbiting molecular reservoirs around many evolved stars. A nice review is by Jura (1999).

CO imaging observations generally support the isotropy of AGB-star outflows. TT Cygni, an AGB carbon star, shows a nearly perfect spherical (albeit clumpy) thin bubble of CO expanding at 12.6 km s^{-1} with a mass of 0.007 $M_{\odot}$ and a expansion age of 7000 y if no ambient gas of low specific momentum has been accreted (Olofsson et al. 2000). U Cam has a similar but younger (800 y) bubble-like shell (Lindqvist et al. 1999). IRC + 10420 may be similar (Castro-Carrizo et al. 2001). An exception to isotropic outflow is the carbon star V Hydrae. Kahane et al. (1996) and Knapp et al. (1997) argue that its observed CO profile shapes are best fitted with a tilted equatorial disk expanding at 15 km s^{-1} and collimated outflows of 45 and 200 km s^{-1} along its symmetry axis.

Interestingly, although the vast majority of scattered starlight from IRC + 10216 comes from the many concentric shells in its extended halo, a short exposure HST image shows that the nuclear region has bipolar symmetry (Kwok 2000). Apparently the mode of mass loss in this object has recently changed.

Morphologies of pPNe with Post-AGB Nuclei

Meixner et al. (1997, 1999) have been systematically imaging pPNe in the mid-IR where extinction is probably not significant (but the contribution from cold dust—probably containing a majority of the dust's mass—is minimal). [See the comprehensive review of these surveys by Meixner (2000).] Several very significant results are these: 33 of 73 pPN candidates were spatially resolved, and all of

them are axisymmetric. The mid-IR morphologies of pPNe split into two distinct groups, SOLE and DUPLEX, which are possibly the antecedents of elliptical and bipolar PNe, respectively, though there is disagreement on whether these groups are truly distinct or just the result of inclination effects.

Some spectacular individual cases of highly collimated outflows, many showing shock-excited optical emission lines, have been studied in the papers listed earlier. The lobes of He3-401 show magnificent pencil-like collimation very clearly traceable to a central disk (Sahai et al. 1999a). Kwok et al. (2000) uncovered a spectacular example, IRAS 17106-3046, which clearly shows a bipolar outflow along the symmetry axis of a disk seen clearly in reflected light. IRAS $04296+3429$ may be a very similar structure (Sahai (1999). [See the bottom row of Figure 1 for selected images.]

Kinematical studies of post-AGB nebulae are generally made in the bright low-lying transitions of CO. Early single dish observations showed that most pPNe have an integrated CO profile that has a Doppler half width of 15–30 km s^{-1} (Huggins & Healy 1989). Recently CO interferometer maps have revealed unexpected details (e.g., Alcolea et al. 2000). Deeper, higher-transition CO lines occasionally show additional broad ($\geq$100 km s^{-1}) faint wings (Bujarrabal et al. 2001). Of those that have been imaged in CO, virtually all are butterfly pPNe. The most notable are CRL 2688, CRL 618, OH231.8 + 4.2 (Figure 1), M1–92, and He3–1475 (Figure 1), in no particular order. Each is a highly individualistic case. Some show optical emission-line radiation, generally from shocks, which allows their morphology and kinematics to be traced in great detail.

In summary, although pPNe associated with AGB stars are normally round, those of post-AGB objects are largely axisymmetric and those of high-luminosity systems are often highly bipolar. It is easy to conjecture that the halos of ordinary PNe form first and then the mode of mass loss changes to axisymmetric. Indeed, the images of young PNe by Sahai & Trauger suggest that the new mode of mass loss is one of very carefully orchestrated outflow patterns that soften considerably as photoheating and ionization fronts alter the nebula.

Outflow Momenta of pPNe

We highlight a very important kinematic result that has not received adequate attention: Radiatively accelerated winds cannot account for the momenta implied by the broad wings of the CO profiles of pPNe with relatively high-mass nuclei. This problem was identified first by Knapp (1986), and most recently and comprehensively investigated by Bujarrabal et al. (2001). The latter summarize the CO data for 16 objects that they studied and another 21 objects compiled from the literature.

Almost 90% of 32 objects with excellent data show optically thin, broad wings containing at least 0.1 $M_\odot$ of gas. By taking the first moment of the line profile, Bujarrabal et al. 2001 computed the component of momentum along the observer's line of sight (a fraction of the total momentum, of course). As discussed earlier, this scalar momentum P can be compared to the momentum in the stellar radiation,

$(L_*/c)\Delta t$, where here L_* is the stellar luminosity emitted during the pPNe outflow expansion lifetime, Δt. They find that after conservatively culling objects for which data are dubious, 21 of 23 CO-emitting pPNe with high-mass central stars show highly excessive (factor of >100) outflow momenta. The excess momentum was not seen in any of the four low-mass stars in their survey. In light of these results, both the launching and collimation of winds in pPNe becomes problematic.

Two Case Studies

A detailed understanding of exceptional objects may be useful for uncovering and evaluating the key physical processes involved in a class of objects. Therefore we present the observational results of two case studies of phenomenological extrema in which the shaping processes act with outstanding vigor. We elect to consider OH231.8 + 4.2 (a.k.a., the Calabash or Juggler or Rotten Egg Nebula, OH07399–1435, QX Pup, CRL 5237) and He3–1475 (a.k.a. Henize 3–1475, IRAS 17423-1755). Both show strong IR excesses, shock-excited optical emission line nebulosity, very fast outflows (300 km s^{-1} for OH231 and 2000 km s^{-1} for He3–1475), and highly bipolar (butterfly) structures. Images of both nebulae are found in Figure 1.

OH231.8 + 4.2 The nucleus of OH231 is QX Pup, a 700-day variable Mira of spectral type M9III (Cohen 1981). A slowly expanding SO disk seems to surround the nucleus (Sánchez Contreras et al. 2000b). Evidence of binarity was found by Gómez & Rodgríguez (2001), who suggest that the lobes originate $\sim 1''$ from QX Pup at a putative invisible companion in a torus-like region of very high extinction. Obviously the nucleus may be a symbiotic star.

OH231 exhibits two closed, edge-brightened, seemingly hollow lobes seen in Hα, [N II], and other low-ionization optical lines (Sánchez Contreras et al. 2000a and Reipurth 1987). As seen in Figure 1, the southern (receding) lobe is twice as large but fainter in surface brightness than its northern counterpart. Two finger-shaped columns seen in dust-scattered starlight and molecular line emission span the lobes from the nucleus to the outermost lobe tips along the nebular symmetry axis. Optical emission lines and HCO^+ peak at the outer tips of the lobes where these lines are probably excited by local shocks, as outflowing gas flowing along the fingers splashes into the lobe edges (Sánchez Contreras 2000a).

Alcolea et al. (2001) mapped the distribution and kinematics of CO in the fingers of OH231. One third of the total CO mass of 1 $M_\odot$ is associated with the fingers, and the rest is concentrated close to the nucleus. The CO Doppler shift increases linearly with distance from the nucleus along the fingers to -210 km s^{-1} at the tip of the northern lobe and $+430$ km s^{-1} in the southern, suggesting a single expansion age of 780 y for both lobes. Thus, the collimated fingers may have been produced in a brief but highly organized event. (We hasten to add the pPN M1–92 and the bipolar PN He2–104, each with a symbiotic/Mira nucleus, share many morphological and kinematic similarities with OH231.) Another key point

raised by Alcolea et al. is that the excess of scalar momentum observed in the CO outflows is far too high—by a factor of 1000—to be explained by the momentum carried by radiation pressure.

He3–1475 Riera et al. (1995) (hereafter RGMPR95) first called attention to this remarkable Pop II object that lies in the bulge 800 pc above the Galactic nucleus where its luminosity is $2 \cdot 10^4$ $L_\odot$ (Borkowski & Harrington 2001; BH01). RGMPR95 found that P-Cyg features and strong permitted lines such as FeII and CaII arise in the nucleus, suggesting a B[e] or B[q]-type nuclear spectrum. They also found near-nuclear knots with outflow speeds, which, after an uncertain correction for inclination, imply outflow speeds of 2000 km s^{-1}. BH01 and Sánchez Contreras & Sahai (2001) (SS01), using HST spectra with $\sim$0.05″ spatial resolution, resolved individual knots of high-speed outflows, one characterized by 1200 km s^{-1} within $5 \cdot 10^{16}$ cm of the nucleus, and the other by 2300 km s^{-1} within 10^{16} cm.

RGMPR95 were also the first to note that much of the forbidden line emission (largely [NII]) arises from a series of N-rich knots emanating along an S-shaped (point symmetric) axis through the nucleus. The knots have decreasing densities, very high electron temperatures ($\sim$18,000 K) and line splittings consistent with fast-moving and expanding blobs excited by local shock heating. The Doppler shifts of the knots steadily decrease with radius, which is highly unusual among bipolar PNe and pPNe. RGMPR95 suggested that the knots are ejected from a precessing "cannon" anchored to the nucleus. If so they must decelerate as they propagate in order to prevent merging.

HST images by Borkowski et al. (1997 hereafter BBH97) spatially resolve the knots and some of the bow shocks along with a thick dusty torus associated with the nucleus. One of the innermost knots is seen to have an outward-facing arrow-like shape. However, SS01 assert that the streamlines of 2300 km s^{-1} outflow appear to be pristine stellar winds that emerge fully collimated from the unresolved nuclear region.

Single-dish CO observations of He3–1475 were reported by Bujarrabal et al. They show relatively broad ($\sim$50 km s^{-1}) but weak emission wings. Bujarrabal et al. find a CO mass of about 0.6 $M_\odot$ and a large excess (1000) of scalar momentum over that expected from the cumulative pressure of stellar radiation.

OBSERVATIONAL RESULTS AND QUESTIONS: SUMMARY

A summary list of results and unresolved issues posed by observations makes a nice transition from the observations reviewed in "Classical PNe" and "ProtoPNe" to theories and paradigms starting in "Variations on a Theme: Theoretical Models".

- The morphologies of PNe and pPNe consist of three major types: round, elliptical, and bipolar, all of which normally show reflection symmetry about

their major and minor axes. We further distinguish butterfly bipolars with strongly pinched waists from bilobed bipolars containing an elliptical core. A small fraction of PNe show point reflection through their nucleus, and some bipolars exhibit multiple axes of axisymmetry. Is there a single unified model/paradigm that can explain the large-scale shapes of pPNe and PNe, or is more than one set of shaping processes universally at work?

- Disks and tori are nearly ubiquitous among PNe and pPNe (other than round ones). What process or processes produces these structures?
- The outflows in butterfly PNe and pPNe can sometimes be highly collimated. Does the inertial pressure of a dense equatorial disk or torus serve as a collimation nozzle? Or are the flows collimated by magnetic forces or by accretion from a companion star?
- Many PNe and pPNe exhibit kinematic patterns that are readily assignable to Hubble Flows (expansion speed $\propto$ radius). What does this infer about the ejection and/or expansion of the nebular material? Are the motions ballistic (i.e., nonhydrodynamic) or self-similar (in which hydrodynamic shaping establishes a constant shape which simply magnifies in time)?
- The GISW paradigm has been successful for explaining the large-scale shapes and kinematics of round, elliptical, and bilobed PNe. In stark contrast, most butterfly PNe—which are generally associated with symbiotic stars and/or massive nuclei—attain their shapes in a brief event and then seemingly expand ballistically. What is the nature of the event that drives these outflows? Do some PNe avoid hydrodynamic shaping altogether?
- pPNe surrounding AGB stars tend to be isotropic, whereas those around the nuclei of post-AGB pPNe are highly axisymmetric. The change in morphology may be associated with a qualitative change in their IR colors and SEDs during the transition from AGB to post-AGB states. Abrupt changes in the mode of mass loss appear at about this state in the evolution of PNe. All of these results provide circumstantial evidence for the formation of a cool, dense disk/torus at the AGB–post-AGB transition. What process or processes drive the mode change?
- Outflows are generally believed to be the results of radiation-driven stellar winds. Yet many pPNe with relatively high-mass nuclei exhibit momenta orders of magnitude greater than stellar radiation pressure can provide during the expansion lifetime of the outflow. Do the nebular momentum excesses imply that bipolar pPNe are formed by highly disruptive events?
- A small but significant subsample of PNe and pPNe exhibit S-shaped (point-symmetric) morphologies or multiple lobe symmetry axes. It has been suggested repeatedly that the flow collimator precesses or becomes unstable in these systems. How is the collimator destabilized? Is it related to tidal disruption or merger of a companion star? Are magnetic or disk instabilities potentially important?

- YSOs, some LBV nebulae, and some AGN outflows share some striking morphological similarities with their brighter, less obscured counterparts, PNe and pPNe. What shaping processes do they share in common?

Observational Support for Collimation Mechanisms

Producing any preferred axis of mass ejection and symmetry is a nontrivial problem for isolated AGB stars. The two most obvious ways to impose a preferred axis are rotation and/or surface magnetic fields. However, the angular momentum needed to distort a star's surface or form a stable disk are at least two orders of magnitude larger than the angular momentum in the Sun (Wood 1997). Models that require rotation to near-breakup speeds are not plausible without accounting for special sources of angular momentum (see below.)

The recent literature is replete with suggestions that either interacting binary systems or magnetic fields must be the agent(s) that collimate outflows. Are these suggestions backed by direct evidence, circumstantial arguments, or merely speculation? We end this section by addressing the observational evidence for closely orbiting companions and magnetic fields. The putative shaping effects of fields and companions are discussed later.

BINARITY AND RAPID ROTATION IN THE NUCLEI OF PNe Livio, Soker, and many others have long pointed out that the loosely bound envelope of an AGB star is particularly susceptible to external torques or tidal forces exerted by a nearby orbiting companion. Extremely close companions can lead to mass transfers and the formation of an accretion disk on the secondary. Mergers can spin up the AGB star to breakup, rapidly initiating various disk-forming processes in its newly bloated outer layers. Companion stars potentially solve a host of awkward problems—but only if they actually exist.

Let us consider the evidence of frequent binarity in AGB stars that might account for the statistical properties of PN asymmetries. Only 16 Galactic PNe are observed to have close binary nuclei (Bond 2000). On the other hand, companions may quickly merge as the energy and angular momenta of their orbits are transferred to the AGB star, leaving no remaining trace of binarity by the time asymmetries are visible in the nebula. Indirect evidence of recent mergers would be rapid rotation in AGB stars. However, Barnbaum et al. (1995), in a study of 74 carbon stars, found only one, V Hydrae, with detectable rotation (which they attribute to mass transfer from an unseen companion). Interestingly, V Hya and perhaps IRC + 10216 are unusual AGB stars that show strong signs of collimated outflows.

The strongest arguments for companions are by Yungelson et al. (1993) who were the first to show theoretically that the expected frequency of binarity in the nuclei of PNe is consistent with the histograms of PN morphological types. Their results were corroborated and extended by Soker & Rappaport (2001). Observationally, Wood et al. (1999) found that 25% of the AGB stars in the LMC bar are variable. They ascribe the variability to mass transfer from the AGB star to an

invisible companion in a semidetached binary. These results agree well with predictions by Han et al. (1995): 30–40% of stars could experience mergers on the AGB.

Soker (1998a) made a critical observation: the outflow speeds of most highly collimated PNe, often hundreds of km s^{-1}, is far more than a factor of ten larger than the escape velocity from the surface of an AGB or post-AGB star. He suggests that these speeds can only be obtained in close binary systems with high orbital speeds. As we have seen, the outflow momenta of luminous pPNe are far too great to have been produced by stellar radiation pressure, perhaps also suggesting that the system must extract this excess momentum from a closely orbiting companion.

The bottom line is that although binarity is a popular mechanism for forming axisymmetric structures on PNe, direct evidence to support the efficacy of the process is not strong. However, the indirect evidence for binarity in highly bipolar PNe is rather suggestive but still far from compelling.

MAGNETIC FIELDS IN PNe The role of magnetic fields in shaping PNe is under increasing consideration, as described in later sections (García-Segura et al. 1999, Frank 2000). In order to be effective, the energy density of the fields must be equal to or surpass that of thermal pressures and bulk motions in the outflowing winds. Models described below require at least a magnetic field strength of a gauss at or near the stellar surface. Are such fields common? Do fields play their role close to the star where they would be much stronger or do magnetized winds sweep into the nebula where the tension of the fields can deflect streamlines?

The evidence in favor of fields is sparse, particularly in ionized gas where thermal broadening renders any search for Zeeman splitting hopeless. Even in neutral gas such fields are very difficult to detect because detectable synchrotron and cyclotron emission is not expected, and any polarized line radiation is swamped by brighter foreground and background gas. So far, the evidence for magnetic fields is limited to the high degree of circular polarization found in OH masers. Palen & Fix (2001) found 100% circular polarization in some OH-IR stars, requiring the Zeeman splitting associated with at least a milligauss field in the maser path. Recently, Miranda et al. (2001a) examined a young PN K3-35 and found partial circular polarization of OH masers in its disk and at the tips of its butterfly lobes that they also ascribe to magnetic fields.

In short, observations weakly support the notion that orbiting companions and/or magnetic fields can strongly influence the shaping of PNe. The biggest problem is the extreme difficulty of direct and decisive measurements. The paucity of evidence provides theoreticians with an unconstrained opportunity to model how companions and fields—or any other mechanisms—might serve as shaping tools without the fear and useful feedback of embarrassment.

VARIATIONS ON A THEME: THEORETICAL MODELS

In the second half of this paper, we review theoretical models that attempt to explain the shapes and shaping of PNe and pPNe. It is the close coupling between rapid variations in the evolution of the star and the processes of nebular shaping

that makes these objects so interesting from a theoretical standpoint. Whereas radiation-(magneto)hydrodynamic models of nebular evolution may give shapes and kinematics that match observations, a truly successful model must also account for the model's initial conditions that are ultimately associated with the evolution of the star. At present, this is just a hope. This lack of unification in stellar and nebular evolution represents one of the greatest challenges facing the field.

Before launching into the theoretical details of this section, of which there are many, it is important to provide a sense of structure for the discussion. The primary goal is to identify workable, effective physical mechanisms that are grounded in well-understood astronomical contexts. These must explain deviations from isotropic outflows during the formation and evolution of PNe. Thus, we build a foundation based on simple physical models and the results of their numerical derivatives. At the end we present and evaluate specific collimation concepts. Along the way, however, we address several of the questions and challenges posed in "Observational Results and Questions: Summary," such as the formation of knots and jets, the effects of magnetic fields, close companion stars (including those that form common envelopes), ionization fronts, rapid stellar rotation, etc.

Basic Models: Physics, Initial Conditions, and Equations

The published theoretical work on pPN/PN shaping falls into two broad categories: inertial confinement and self-confinement.

INERTIAL CONFINEMENT MODELS In GISW models a fast wind from the central star of a pPNe or PNe expands into an environment created by an older slow wind whose density distribution is assumed to be toroidal. The essence of this mechanism is basically gas bouncing off a pre-existing equatorial wall of some kind. Note that most GISW models are incomplete because they do not specify how the aspherical environment was created. Popular models for creating the torus are discussed elsewhere in this section.

SELF-CONFINEMENT The variety of nonaxisymmetric features observed in PNe over the past decade, such as point-symmetric jets, have led to the emergence of a different class of theoretical models in which the wind from the central star is self-collimated. The published models to date have all relied on magnetic fields embedded in the wind to achieve this collimation. The use of MHD effects to create various classes of features begs the question of how the fields are created. This is similar to the way GISW models ignore the origin of toroidal ambient density distributions. Thus, once again, there is a division between models that explain the shapes of pPNe and PNe and those that attempt to explain the origin of the initial conditions that allow the nebular MHD models to operate. A schematic overview of various pPNe and PNe shaping mechanisms is shown in Figure 2 and described in its caption.

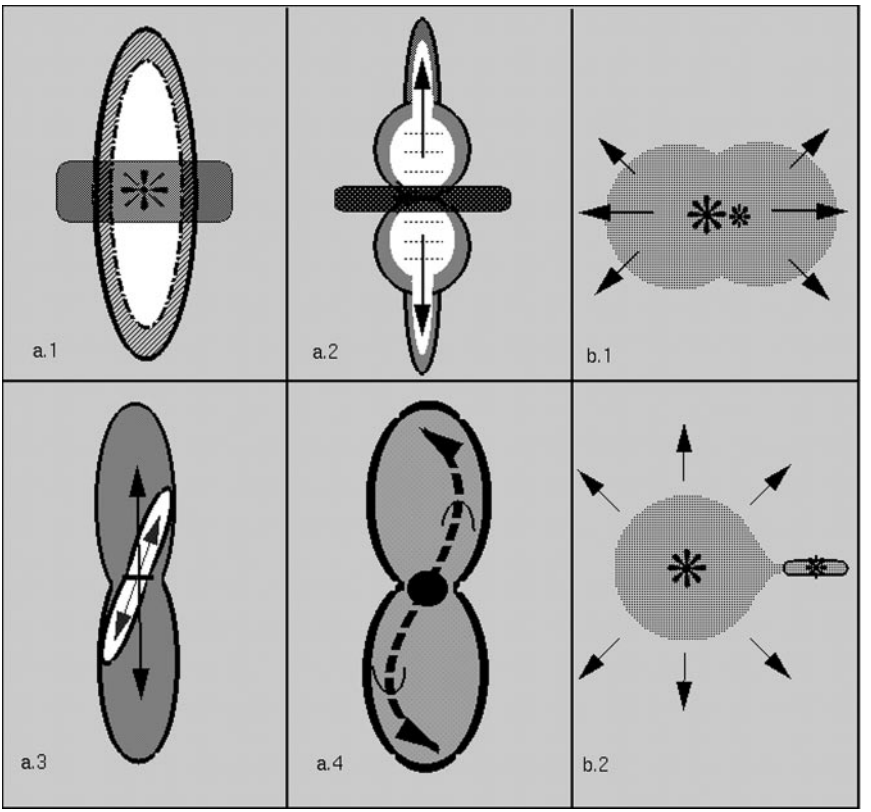

Figure 2 Set of six schematic diagrams showing possible pPNe and PNe formation mechanisms. Schematic a.1 represents the Generalized Interacting Stellar Winds model (GISW) in which an isotropic fast wind from the star expands into a previously ejected toroidally shaped slow wind (Icke et al. 1989, Mellema & Frank 1995). Schematic a.2 represents the Magnetized Wind Blown Bubble (MWBB) in which a weakly magnetized fast wind expands into an aspherical density distribution (Chevalier & Luo 1994; García-Segura et al. 1999). Toroidal magnetic fields (*dashed horizontal lines*) strengthened after passage through the inner shock constrain the outflow and produce jets (*arrows*) along the axis. Schematic a.3 represents disk/star magneto-centrifugal models. A rapidly rotating central object (a disk and/or a star) launches a wind that collimates via hoop stresses. Misalignment of disk and star rotation axis produces multipolar lobes (Blackman et al. 2001a). Schematic a.4 represents outflows driven by episodic jets (collimated on unresolved scales). Precession of the episodic jet can create point symmetric nebulae with interior bow shocks (Cliffe et al. 1996, Steffen & López 1998, Soker & Rapport 2001). Schematic b.1 and b.2 represent processes that can create the toriodal slow wind. Schematic b.1 represents common envelope evolution for short period binaries (Soker 1997, Rasio & Livio 1996). Schematic b.2 represents accretion disk formation via Bondi accretion and Roche lobe effects (Mastrodemos & Morris 1999).

BASIC PHYSICAL ELEMENTS In studying the shaping of PNe the theorist's task is to track an outflow driven by a star embedded in some form of ambient medium. The structure of the theory is built on the equations of mass, momentum, and energy conservation. The first task is to identify the physical processes that need to be included in the equations. As already noted, magnetic fields may play a dynamically significant role. Thus we need to model a multidimensional, time-dependent MHD flow. We should also include heating and cooling of the gas due to radiation. A proper treatment of energy source terms requires calculation of the microphysical state (ionization, chemistry, level populations). Radiation transfer should be treated explicitly.

The hydrodynamic equations written with the correct microphysical terms and radiative transfer equations can be found in (Frank & Mellema 1994a, Marten & Szczerba 1997). The relevant form of the ideal MHD equations can be found in many references (Priest 1984, Choudhuri 1998). In solving the hydro/MHD equations for pPNe/PNe, many authors have neglected dissipative processes such as molecular and turbulent viscosity, and heat conduction and resistivity. In some settings these processes, particularly heat conduction, may become important (Weaver et al. 1977, Soker 1994a, Kastner et al. 2000). Resistive processes can drive reconnection events in the flow and may be important since they convert magnetic into thermal energy while altering magnetic field topologies.

Hydrodynamic Models of Inertial Confinement

SPHERICAL INTERACTING WINDS MODELS The majority of hydrodynamic theories of PN shaping are based on a generalization of the interacting stellar winds model for PNe that was first applied to PNe by Kwok et al. (1978). We first consider the theory for spherical, hydrodynamic ($\mathbf{B} = \mathbf{0}$) wind-blown bubbles to clarify basic dynamical issues. In what follows we borrow liberally from a number of excellent treatments of spherical wind-blown bubble theory (Dyson & de Vries 1972, Weaver et al. 1977, Dyson 1977, Kwok et al. 1978, Dyson & Williams 1980, Koo & McKee 1992, Kahn 1983). A more complete version of this review of hydrodynamic shaping appears in Frank (1999).

When a stellar wind is initiated it expands ballistically from the source until enough ambient material is swept up for significant momentum to be exchanged between the two fluids. A triplet of hydrodynamic discontinuities forms defining an interaction region bounded internally (externally) by undisturbed wind (ambient) gas. At the outer boundary of this region is an outward-facing shock called the ambient shock at position R_{as}. The inner boundary is defined by an inward-facing shock called the wind shock at position R_{ws}. A contact discontinuity (CD), R_{cd}, separates the shocked wind and shocked ambient material. In a spherical bubble [one-dimensional, (1-D)] these discontinuities form a sequence in radius: $R_{ws} < R_{cd} < R_{as}$.

The compressed gas behind either or both shocks will emit strongly in optical, UV, and IR wavelengths producing a bright nebular rim that defines the observable

bubble. The dynamics of the bubble will be determined by the strength of post-shock cooling. We can define a cooling timescale $t_c = E_t/\dot{E}_t$ for each shock, where E_t is the thermal energy density of the gas. $\dot{E}_t \propto n^2\Lambda(T)$ when $\Lambda(T)$ is an appropriate cooling curve. Thus, $t_c \propto T/n\Lambda$. We also define a dynamical timescale $t_d = \frac{R_{as}}{V_{as}}$, where V_{as} is the speed of the ambient shock. Comparison of t_c and t_d then separates wind-blown bubbles into two classes: radiative (also known as momentum conserving) and adiabatic (a.k.a. energy conserving).

In PNe and pPNe, the densities in the ambient medium (the slow AGB wind, a circumbinary torus, etc.) are high enough to ensure a radiative ambient shock. Thus, $R_{as} \approx R_{cd}$ and the bubble will have a thin outer rim. The cooling properties of inner shock, however, can vary, and these changes can determine the bubble's dynamics. If $t_c > t_d$, the cooling is weak. The gas retains thermal energy gained after passing through the shock transition, and a hot bubble forms. This type of shock is sometimes referred to as adiabatic. High pressure behind an adiabatic shock limits gas compression ($\rho_{post} \leq 4\rho_{pre}$). In the co-moving frame of the CD, the wind shock is pushed back toward the star, $R_{ws} \ll R_{cd}$. In these adiabatic or energy-conserving bubbles, it is the thermal energy (pressure) of the shocked wind that drives the expansion of the bubble as a whole.

If $t_c < t_d$—which generally applies to pPNe for which the speed of the fast wind is under 150 km s^{-1}—then the gas cools quickly relative to the bubble's growth. The loss of thermal energy behind a strongly cooling radiative shock means the loss of pressure support as well. Because its internal energy is quickly converted into escaping radiation, the shock collapses back toward the contact discontinuity (in a frame moving with the shock). A thin dense shell forms with $R_{ws} \approx R_{cd}$. The expansion is now driven directly by the ram pressure of the stellar wind $\rho_w V_w^2$, and the bubble is often referred to as wind driven, momentum conserving, or radiative. At higher fast-wind speeds, the shocked gas becomes too hot to cool efficiently, so a hot bubble grows between R_{ws} and R_{cd}.

The expansion speed of pressure-driven and wind-driven nebulae can be determined through either exact solutions (Koo & McKee 1992) or through dimensionless arguments. Beginning with a generic spherically symmetric environment $\rho(R) = \rho_0 R^{-l}$, and a wind with mechanical luminosity $L_w = .5\dot{M}_w V_w^2$ (or momentum input $\dot{\Pi} = \dot{M}_w V_w$), one finds the following expressions for the radius of energy- and momentum-conserving systems:

$$R_{as}^E(t) \propto \left(\frac{L_w}{\rho_0}\right)^{\left(\frac{1}{5-l}\right)} t^{\left(\frac{3}{5-l}\right)}, \quad R_{as}^M(t) \propto \left(\frac{\dot{\Pi}}{\rho_0}\right)^{\left(\frac{1}{4-l}\right)} t^{\left(\frac{2}{4-l}\right)}. \tag{1}$$

The first derivative of these expressions gives the expansion speed of the ambient shock. An important point to note here is that the velocity of the ambient shock and nebular rim will be constant for an environment created by a previously deposited wind $l = 2$. Thus wind-wind interactions, which characterize much of PNe and pPNe dynamics, will naturally produce flows that mimic Hubble-law kinematics.

ASPHERICAL NEBULAE—THE GISW MODEL The ISW paradigm can be extended to embrace elliptical and bipolar nebulae by generalizing the model to include aspherical environments. Most work has focused on toroidal density distributions, $\rho(R, \theta)$, with an equator-to-pole density contrast, $q = \rho(0^\circ)/\rho(90^\circ) = \rho_e/\rho_p$, and $q \geq 1$. An isotropic stellar wind encountering inertial gradients in the gaseous toroid will drive an ambient shock that expands more rapidly along the poles than the equator. In his study of energy-conserving GISW dynamics, Icke (1988) showed that

$$\frac{\partial R_{\rm as}}{\partial t} \propto \left\{ \frac{\gamma + 1}{2} \frac{P_{\rm hb}}{\rho_0(\theta)} \right\}^{\frac{1}{2}}. \quad (2)$$

Although the pressure in the hot bubble P_{hb} is nearly constant, Equation 2 shows that the angular variation of $\rho_0(\theta)$ determines the asphericity of the nebula. It is, therefore, the inertia in the ambient medium that determines the shape of the bubble. We note that in these models, the ambient thermal pressure plays no role in the collimation (Reipurth & Bally 2001).

Analytical determination of aspherical wind-blown bubble evolution involves solving partial differential equations in two spatial dimensions and time, and it remains a difficult problem. Dyson (1977) and Kahn & West (1985) provided analytical solutions for GISW bipolar energy-conserving nebula. Icke's (1988) investigation explored a wider range of solutions demonstrating that strongly collimated solutions for $R_{as}(\theta, t)$ could be generated if the torus had a narrow opening angle. Icke et al. (1989) also provided synthetic observations of such models. In a study of R Aquarii, Henny & Dyson (1992) used a model based on momentum conservation in the shell and included emission characteristics of the bubble for both shock-excited and photoionized emission. Working off a novel method proposed by Giuliani (1982), Dwarkadas et al. (1996) produced similarity solutions for bipolar wind-blown bubbles. These solutions predicted not only the shape of the bubble, but also the mass motions along the shell of swept up ambient gas that can lead to substantial modifications of shell density.

Any study of the GISW formalism must include specification of the ambient density distribution. The majority of GISW models of PNe assumed ad hoc forms for the ambient density: $\rho(r, \theta) \propto R^{-l} F(\theta)$ (Dwarkadas et al. 1996). More recent studies (García-Segura 1997, García-Segura et al. 1999, Collins et al. 1999) have attempted to incorporate specific physical models for the creation of the toroidal environment into GISW calculations. This appears to be one of the most important paths for future research.

NUMERICAL MODELS The inherent complexity of the GISW problem make simulations a necessary tool for explicating the true range of hydrodynamic flow patterns. One-dimensional spherically symmetric numerical models have reached a fairly high degree of sophistication in terms of their treatments of both hydrodynamics, radiation transfer, and microphysical processes (Frank 1994, Mellema 1994, Arthur et al. 1996, Steffen & Schönberner 2001). Recent 1-D models have

made significant steps linking stellar and nebular evolution models (Schönberner & Steffen 2001). Multidimensional studies have been more limited in their ability to link source physics to the nebular evolution.

Soker & Livio (1989) were the first to explore time-dependent GISW simulations of bipolar PNe. Using higher-order methods and higher-resolution grids, Mellema et al. (1991) and Icke et al. (1992) explored the hydrodynamic flow pattern in bipolar wind-blown bubbles in more detail. They provided an extensive mapping of parameter space and articulated the dynamics of the ambient/wind shocks in greater detail. The formation of highly collimated supersonic jets inside the hot bubble was one of the most surprising results of these simulations.

Radiative losses were included in a series of studies by Frank & Mellema (Frank & Mellema 1994a,b; Mellema & Frank 1995; Mellema 1995) who developed a 2-D numerical code including hydrodynamics, microphysics, and radiation transfer from the hot central star. These models tracked cooling and emission behind the ambient shock and explored the limits, in terms of pole-to-equator density contrast q, of the nebular shaping. For low values of q, ($q < 2$), the results showed bubbles become mildly elliptical. Intermediate values of q, ($2 < q < 5$), produce distinct equatorial and polar regions of the ambient shock; i.e., bipolar lobes develop. Larger values of q produce bubbles that are highly collimated. The inclusion of radiative loss terms allowed confrontation with observations of both morphology and kinematics. The models were successful at recovering many of the observed morphological, kinematic, and ionization structures seen in a considerable range of elliptical and some bipolar PNe. Figure 3 compares the results of a GISW model along with synthetic observations with real data for NGC 3242.

Dwarkadas et al. (1996) explored the effect of slow wind speeds on bipolar PNe evolution. Their results demonstrated that the effects of a density contrast in the ambient medium can be washed out when ambient shock and slow wind velocities are comparable. This occurs because the bubble shell is always catching up to the slow wind and no inertial constraint can be imposed.

Dwarkadas et al. also provided the most detailed comparison between numerical simulations and self-similar analytical models available to date. Their results confirm that the two approaches yield similar bubble shapes when the hot bubble remains isobaric ($P_{HB} \approx Const.$). This isobaric condition then determines when energy-conserving bubbles will achieve Hubble-Flow kinematics.

THEORETICAL MODELS AND HUBBLE FLOWS In "ProtoPNe" we emphasized that many, if not most PNe and pPNe are characterized by uniform, homologous expansions that we described as Hubble Flows. We noted that such kinematic patterns could be the result of ballistic motions or self-similar hydrodynamic growth patterns. Hydro models of radial outflow from a central source have a natural tendency to settle into self-similar growth. As noted above, the underlying reason is that when the fast and slow winds are largely radial, geometric dilution in consort with conservation of mass and momentum densities tend to relax nebular shapes to configurations where $v(r)$ (at each latitude) is constant. This behavior may only be modified by aspherical shock effects.

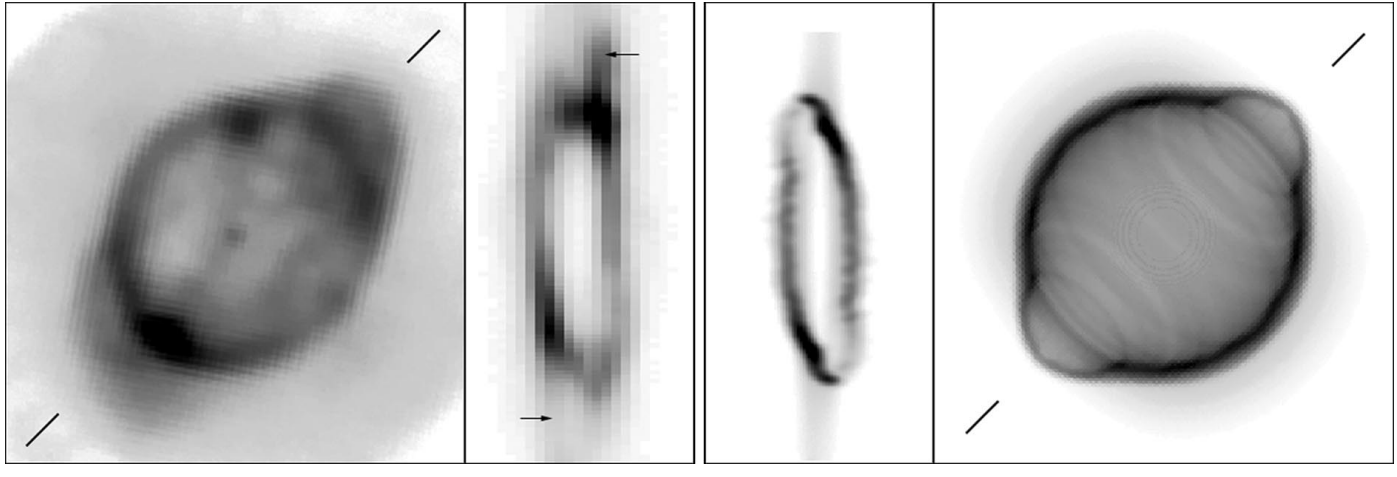

Figure 3 Morphologies and kinematics of GISW model: comparison with reality. *Left*: [OIII] image of NGC 3242 (Balick 1987) along with long slit echelle spectra along major axis (Y. Chu & Jacoby, personal communication). Solid lines mark the location of the Echelle slit. Arrows point to features related to the FLIERs of NGC 3242, which are not a part of the model shown to the right. *Right*: Corresponding synthetic [OIII] image and kinematic from a purely hydrodynamic model of a fast wind expanding into a toroidal slow wind with moderate density contrast. [For more details see Frank & Mellema (1994b)]. Some panels have been modified with permission of the authors.

Which Hubble Flows are ballistic or self-similar? The primary difference between the two types of Hubble flows will be the presence of large-scale working surfaces, such as prolate elliptical or peanut-like shocks, which will indicate whether hydrodynamic shaping is globally active. Observationally, we might expect to find dense filaments of atypical ionization or regions of abrupt changes in kinematics where pressures across these surfaces are actively shaping the nebula.

THE ROLE OF IONIZATION The toroidal circumstellar environment it is likely to form before the star produces significant UV flux. Thus, nebular shaping begins while the torus is still neutral and cold. Mellema (1997) included evolution of stellar ionizing flux in bipolar PNe simulations and found that rapidly evolving, higher-mass stars ionize the entire environment on timescales $<t_d$. Lower-mass stars tend to have ionization fronts (IFs) in their nebulae for longer periods of time. In addition, ionization of high q environments lead to latitudinal pressure gradients. In these systems, the effective q drops with time leading to more elliptical PNe.

Trapped ionization fronts can also lead to instabilities of various types including Rayleigh-Taylor modes. Analytical models including time-evolution of both the wind and the ionization flux were calculated by Breitschwerdt & Kahn (1990) and Kahn & Breitschwerdt (1990) who showed that a brief period of ionization-front trapping could drive instabilities. García-Segura et al. (1999) have published results showing instabilities in the nebular rim that appear to occur directly from local variations in ionization fractions. Thus, stellar UV photons can affect both the global properties of the flows as well as the development of micro-features. These ionization models may help us to understand how ripples and fingers grow in very young PNe, and may also provide insight into the formation of the serpentine and starfish morphologies of very young PNe ("ProtoPNe").

MHD Models of PN Formation: Self-Confinement

The long lever arm offered by magnetic fields makes them a natural candidate for imposing ordered nonaxisymmetric structures on expanding plasma systems. Delemarter (2000) explored numerical GISW models for CRL 2688 (The Egg Nebula). Numerical simulations (with H_2 and scattered light synthetic observations), showed that a jet, collimated on small scales ($<10^{15}$ cm), was needed to explain the observations. These results indicate that for at least one well-studied object, the GISW model could not capture the proper dynamics.

In their groundbreaking works on jets in PNe, Morris (1987) and Soker & Livio (1994) mapped out scenarios in which accretion disks form around binary PNe progenitors. Each study equated the existence of disks with the existence of jets. The details of the jet launching and collimation mechanism were not, however, specified. Recent work by Soker & Rapport (2001), Soker (2001), and Soker & Livio (2001) have put collimated winds from disks to good use but these works also do not specify how such winds are launched or collimated. As we will see, the twin

concerns of creating the wind and focusing it into a narrow outflow determines much of the current debate on MHD PN models.

A number of MHD models of PNe exist in the literature. Gurzadyan (1997 and references therein) assumed a dipolar field in the nebulae as a shaping agent. In a more recent series of papers, Pascoli (1985, 1992, 1997) explored models where toroidal fields embedded in the previously ejected AGB wind produce the bipolar morphologies. Whereas the Pascoli models have been successful at articulating certain limits of MHD shaping, they have yet to find empirical grounding as an explanatory framework. Currently, two flavors of MHD model appear particularly promising.

THE MAGNETIZED WIND-BLOWN BUBBLE (MWBB) MODEL Motivated to produce bipolar outflows without the need of an inertially confining torus, Chevalier & Luo (1994) developed the MWBB model that relies on hydromagnetic forces in the shocked stellar wind itself. This model assumed a dynamically weak field embedded in a spherically expanding fast wind with foot-points tied to a rotating stellar surface (similar to the Parker solar wind solution). Applying flux conservation gives a poloidal magnetic field B_p that scales as $1/r^2$ and a toroidal field B_ϕ that (for $r \gg R_*$) scales as $1/r$. Here, R_* is the stellar radius. The growth of the toroidal field is directly related to the rotation rate of the star and takes the form $B_\phi = -B_r(\frac{r\Omega\sin(\theta)}{v_r})(1 - \frac{R_*}{r})$.

At large radii the field becomes dominated by the toroidal component $B \sim B_\phi$. When $v_w = Const.$ and $\rho \propto 1/r^2$ the ratio of magnetic to kinetic energy $\sigma = B_\phi^2/(4\pi\rho v_w^2)$ is constant. σ then becomes the principle parameter determining the behavior of the wind driven bubble and can be expressed as,

$$\sigma = \frac{B_*^2 R_*^2}{\dot{M}_w V_w}\left(\frac{V_{rot}}{V_w}\right)^2, \tag{3}$$

where B_*, V_{rot}, and v_w are the stellar radius, stellar rotation rate, and stellar wind speed, respectively. We note that the form $B_\phi \propto r^{-1}$ is a generic feature of toroidally dominated winds even when the field is weak as in this case (Matzner & McKee 1999).

In Chevalier & Luo's MWBB model, the field remains dynamically insignificant until the fast wind passes through the inner shock. Compression then strengthens the field and latitudinal variations in the total pressure $P = P_g + B^2/8\pi$ drive the evolution of globally aspherical morphologies.

Using an analytical formulation with an adiabatic wind shock, Chevalier & Luo demonstrated that magnetic forces in the hot bubble could produce significant departures from spherical morphologies. For a strong bipolar morphology to develop they found that $\sigma > 10^{-4}$.

NUMERICAL MWBB MODELS The first numerical simulations of the MWBB model were carried out by Różyczka & Franco (1996). Whereas these models showed

magnetic collimation in the hot bubble, globally it was restricted to a mild lengthening of the bubble's long axis. More dramatic, however, was the formation of dense, higher velocity features on the poles giving the computed nebula a distinct lemon shape. To achieve this level of magnetic collimation, Różyczka & Franco found $\sigma > 0.05$, i.e., far stronger fields than required for analytical models.

In the case of adiabatic wind shocks and low σ, the long timescales for magnetic collimation are to be expected. In the absence of strong cooling, the plasma beta parameter, $\beta = 8\pi P_{gas}/B^2$, can only increase across a shock (Priest 1984). Globally, magnetic forces in the hot bubble will act on Alfvénic crossing times R_{hb}/v_a, which will be longer than sonic crossing times. Thus, the overall morphology of the bubble will only change after many bubble expansion times. As Różyczka & Franco point out, Chevalier & Luo used a self-similar (scale-free) formulation of the problem, and collimation may simply occur on a larger scale than most observed nebulae when $\sigma < 0.05$.

When cooling is efficient, however, the field is further compressed (along with the gas), decreasing $\beta = 8\pi P_{gas}/B^2$. Once material passes through the wind shock and cools, Lorentz forces are strongly out of balance with gas pressure gradients. If radiative cooling makes $\beta \leq 1$, magnetic forces (hoop stresses) dominate and plasma will be drawn toward the axis in $t < t_d$.

In order to facilitate higher levels of collimation, the MWBB formalism has also been generalized to include a confining gaseous torus (as in the GISW model). García-Segura (1997), García-Segura et al. (1999), and García-Segura & López (2000) have included gaseous tori in their simulations (as well as a simplified treatment of ionization). In general, these models used relatively low fast-wind velocities ($v_w \sim 100$ km s^{-1}) leading to short post-shock cooling times. It is noteworthy that these speeds are more appropriate to the pPN stage than the fully developed PN stage. The explicit form of the gaseous torus was derived via the wind compressed disk model of (Bjorkman & Cassinelli 1993) by assuming high stellar rotation rates and near-Eddington luminosities.

The combination low β in the shocked wind and an inertially confining environment allowed the García-Segura et al. studies to produce a wide variety of nebular morphologies (confirming the feasibility of the Chevalier & Luo scenario). Note that under these conditions the limiting value of the field was $\sigma > 0.01$.

Based on their results, García-Segura et al. (1999) proposed a scheme for the evolution of PNe shapes based on the values of the stellar rotation rate Ω_*. and the magnetic field strength σ. In general, high Ω_*, high B_* central stars produced the highest collimation. This implies higher mass stars are the progenitors of bipolar nebulae (a result that appears to find support in observations).

One of the more striking aspects of the MWB studies has been the results of fully 3-D models (García-Segura 1997, García-Segura & López 2000), which include precession of the star's magnetic axis. The magnetic field at the source provides the needed lever to drive precession in the bubble as a whole. Most importantly, jets form within the bubble and these are observed to precess with the magnetic axis. We take up the issue of jets in a later section noting here that the resulting

shapes in the simulations are similar to point-symmetric morphologies observed in some PNe.

Collimation, Initial Conditions, and Challenges to MWBB Models

Early criticism of the MWB models hinged on both the strength and topology of the field (Soker 1998b, Frank 1999). This criticism holds for all MHD models. It is unclear as yet if field strengths of the order required for the models can be generated in AGB or pPNe or PNe stars. Soker (1998b) raised the issue of field topology because MWBB models require fields to circle the star in the planes parallel to the equator. This is not the case for the solar wind that is composed of distinct field-reversing sectors. The field direction should also change polarity across the equatorial plane making $B_\phi(\theta = 90^\circ) = 0$ where it may be needed most for collimation. Such polarity reversals could also allow reconnection at the equator providing a sink for magnetic energy (Frank 1999). The severity of the above issues, however, remains to be determined.

More important to the explicit application of the model is the issue of collimation in the wind before it passes through the inner shock. This has been investigated by Gardiner & Frank (2001). The MWBB model assumes that the field is weak and can have no dynamical effect on the flow material until it passes through the inner shock. Given typical wind shock and launching scales of $R \geq 10^{16}$ and $R \approx 10^{11}$, respectively, the magnetic field does not affect the flow over at least five orders of magnitude of expansion. A freely expanding magnetized wind must, however, experience an unbalanced Lorentz force associated with the helical field. This force has a component perpendicular to the wind velocity and can be written as

$$\frac{\rho v_r}{r}\frac{\partial}{\partial r}(r v_\theta) = \hat{e}_\theta \cdot \frac{1}{c}(\mathbf{J} \times \mathbf{B}) = \frac{-B_\phi^2 \cot\theta}{2\pi r}. \quad (4)$$

For some length scale and for some range of σ, the fast wind may collimate on its own. Using a perturbation analysis, Gardiner & Frank (2001) demonstrated that significant redirection of streamlines occurs even for weak fields. Their calculation showed deflections of streamlines of $\delta\theta \approx 10^\circ$ to 23° for $\sigma = 0.02, 0.05$, respectively. Thus, the initial conditions used in the MWBB simulations are not likely to be correct.

Finally, the MWBB model addresses only the issue of outflow collimation and not wind launching. Because the field is explicitly assumed to be weak, it cannot help drive the wind (Lamers & Cassinelli 1999). Because many bipolar pPNe may suffer from a momentum excess ("ProtoPNe"), this must be a concern for MWBB models.

Magneto-Centrifugal Models

Momentum excesses have been encountered before in the YSO community (Lada 1985) in studies of molecular outflows. In those environments, magneto-centrifugal

launching from a rapidly rotating magnetized object has became an attractive solution to the problem of launching and collimating the flow. Such models could be applied to pPNe and PNe as well.

Explicit models of magneto-centrifugal launching in PNe systems were made by Blackman et al. (2001a,b) that attempted to explain launching, collimation, and multipolarity. In the Blackman et al. (2001a) scenario, an accretion disk forms around the recently exposed core of an AGB star. The disk forms from companion disruption after the common envelope phase (Soker & Livio 1994, Reyes-Ruiz & López 1999). Blackman et al. (2001b) modeled magneto-centrifugal winds from a central star. These works focused on the magnetic luminosity L_m as the driver for a mechanical wind luminosity L_w in pPNe/PNe systems,

$$L_w \approx \dot{M}_w v_w^2 \sim L_m = \int (\mathbf{E} \times \mathbf{B}) \cdot d\mathbf{S} \sim \int_{R_i}^{R_o} (\Omega R) B_p B_\phi R dR, \tag{5}$$

where B_ϕ and B_p are the toroidal and poloidal field, respectively, Ω and R are the rotational frequency and radius of the magnetized wind source (star or disk). R_i and R_o define the radial boundaries of the wind-producing region.

Using published models for pPNe accretion disk parameters (Reyes-Ruiz & López 1999), Blackman et al. (2001a) calculated $L_m(t)$ for both the disk and the star separately while also accounting for their coupling. The power of each wind evolved along with the disk and the spin-down of the star. Whereas the results showed that either the stellar or disk wind would dominate at any point in time, the energy and momentum flux from the combined wind system was always sufficient to drive observed pPNe and PNe bipolar outflows and perhaps solve the energy and momentum problems (i.e., $L_m \sim 10^{36}$erg/s). Note also that the star will spin-down as angular momentum is transferred, via the field, to the stellar wind. Thus, magneto-centrifugal winds in PNe may offer a natural explanation for the slow rotation of white dwarfs.

Using a dynamo model based on conservation of mass on shells, Blackman et al. (2001) further concluded that once a magnetized pPNe core is exposed via mass loss or binary effects, it will be spinning fast enough to produce a collimated wind regardless of the existence of an accretion disk.

The degree to which a magnetized stellar rotator will collimate a wind driven off its surface has been explored by numerous authors (Weber & Davis 1967, Sakurai 1985). The efficacy of the magnetic rotator can be expressed via a rotation parameter Q (Tsinganos & Bogovalov 2000) given by

$$Q/Q_\odot \simeq 4(\psi_c/5 \times 10^{26}\ \mathrm{G\ cm^2})(\Omega_c/2 \times 10^{-5}\ \mathrm{s^{-1}}) \times (\dot{M}/6 \times 10^{21}\ \mathrm{g\ s^{-1}})^{-1/2}(V/400\ \mathrm{km\ s^{-1}})^{-3/2}, \tag{6}$$

where ψ_c is the magnetic flux at large distances ($\propto BR^2$), V is the outflow speed, and $Q_\odot \sim 0.12$ is the value for the solar wind. In the expression above, the scales have been set using values that may be appropriate to pPNe. For $Q \geq 1$ the system is classified as a fast magnetic rotator and is expected launch a magneto-centrifugal

wind. Note the MWBB model utilizes winds with $Q < 1$. In the $Q > 1$ regime, larger Q values imply more strongly self-collimated outflows (Lery et al. 1998, 1999). In the single star model of Blackman et al. (2001), values of up to $Q/Q_{\odot} \sim 15$ were found, leading to the conclusion that significant MHD launching and collimation is possible in pPNe/PNe systems.

Some fraction of this magnetic energy may also be available to power X-ray emission from the PNe central stars via reconnection-driven flares. X rays have been reported in a number of PNe (Kastner et al. 2000, 2001), and recent observations of X rays in the NGC 6543 (Guerrero et al. 2001, Chu et al. 2001) have provided direct evidence for hard emission from the central star.

Dynamos and the Challenge to the Magneto-Centrifugal Models

Currently, theories of PNe shaping via fast magnetic rotators remain in their infancy. Whereas these models can make quantitative predictions in terms of the evolution, energy, and momentum of the winds, they have yet to produce detailed predictions of nebular shapes either analytically or via numerical models.

The largest uncertainty facing these models is the presence of a strong magnetic field that, most likely, will require some form of effective dynamo. It is encouraging that milligauss magnetic fields have been observed in both AGB and young PNe. But the MHD significance of these fields, so far found only in scattered masers ("Observational Results and Questions: Summary"), is yet to be understood.

Pascoli (1997) published the first dynamo calculation for an AGB star demonstrating the potential efficacy of the classic differential rotation/convection based $\alpha - \Omega$ formalism (Priest 1984) for producing extended fields in evolved stars. An analysis of the dynamo number N_D, (the ratio of field amplification rate to the dissipation timescale), led Soker (2000a) to the conclusion that $N_D < 1$ and that $\alpha - \Omega$ dynamos could not operate in AGB stars. He focused instead on turbulent-based $\alpha^2\Omega$ dynamos and their ability to produce weak fields.

In Blackman et al. (2001b), detailed models of AGB stars (S. Kawaler, personal communication) were used as input to radially averaged $\alpha - \Omega$ studies. These were first calibrated to the solar dynamo. An interface dynamo was found at the base of the convection zone just above the inert CO core with field strength of $1G$ estimated at the AGB surface. These models assumed momentum conservation on shells in the AGB star allowing core contraction and envelope expansion to create the necessary gradients in $\Omega(R)$. Rapid rotation of the core is also needed to drive a magnetized wind once the outer layers are removed. Note that the Blackman et al. (2001) model did not use the field to drive AGB winds. These were assumed to be radiatively driven.

Soker & Zoabi (2002) recently criticized the assumption of zero-angular momentum transfer, arguing that any field extending into the convection zones would spin down (up) the core (envelope). Thus, $\Omega(R)$ would be too flat for $\alpha - \Omega$ dynamos (see also Hager & Langer 1998). This conclusion is unlikely to hold as

strong field lines will collect into flux-tubes that do not provide significant drag in the envelope. In addition, reconnection in the turbulent convective zone will tend to disconnect the flux tubes from their original foot points. In either case, there remains great uncertainty as to which, if any, dynamo model operates in AGB/pPNe/PNe stars. Further work in these evolved star dynamos is one of the more important future areas of theoretical work in the field.

Theories of Nebular Features: Jets, BRETS, FLIERS

It remains unclear the degree to which the linear structures seen in PNe and pPNe are physically similar to continuous hypersonic plasma beams so prominent in YSOs and other astronomical environments (Gonçalves et al. 2001, Livio 2001). The similarities have, however, led some authors to assume the existence of jets and then model bipolar outflows through jet interactions with the surrounding material (Steffen & López 1998, Miranda 1999, Soker 2002). A number of theoretical efforts have also focused the formation of jets in evolved star systems. We consider formation scenarios first.

HYDRODYNAMIC JET COLLIMATION MECHANISMS GISW simulations showed jets could be effectively generated within bipolar nebulae. The collimation relies on the development of an aspherical wind shock to act as a hydrodynamic lens and focus post-shock streamlines toward the axis (Icke 1988). The process, termed Shock Focused Inertial Confinement (SFIC), is robust (Icke et al. 1992) and has been explored in a number of contexts including low- and high-mass YSOs (Frank & Mellema 1996, Mellema & Frank 1997, Yorke & Welz 1996) and relativistic jets from AGN (Eulderink & Mellema 1994). Icke (1988) and Frank & Mellema (1996) presented analytical models of the action of the oblique inner shock demonstrating that even mildly aspherical wind shocks could produce significant flow focusing and supersonic post-shock speeds without a delaval nozzle.

For radiative wind shocks, high compression forms a thin prolate shell of material that streams along the contact discontinuity. This becomes a converging conical flow near the poles redirecting gas into an axial jet (Cantó et al. 1988, Tenorio-Tagle et al. 1988). Mellema & Frank (1997) placed the development of these flows in the context of global bipolar wind-blown bubble evolution. Their simulations demonstrated that such flows may be a natural and robust consequence of wind/ambient material interactions. Borkowski et al. (1997) also performed simulations of winds expanding into pressure stratified environment. Their intent was to model the jets in pPNe He3-1475. Their results, well matched with analytical models, showed the formation of an empty cavity at the base with a narrow jet emanating from the converging flow at the cavity's tip.

In the GISW model, the fast wind encounters a decreasing ambient density with $\rho(R) \propto R^{-2}$. At some finite radius, the wind shock will change from momentum conserving to energy conserving. Jet collimation via converging conical flows may then be followed by an energy-conserving SFIC phase (Mellema & Frank

1997, Frank et al. 1996). Simulations with evolving winds, however, (Dwarkadas & Balick 1998) showed converging flows may be disrupted by instabilities along the walls of the bubble. Thus, the formation of converging flows in wind-blown bubbles remains an open issue. In a fully 3-D situation, the convergence point could be unstable (García-Segura et al. 1997; J. Blondin, personal communication 1998). Recent laboratory experiments using high-energy density plasma machines have, however, created scaled versions of radiative conical flows (Remington et al. 2000, Lebedev 2001). These studies indicate that the convergence point is remarkably stable.

MHD MODELS OF JET FORMATION The natural tendency for toroidal fields to produce collimation flows make them attractive for producing jets (Lynden-Bell 1996). Simulations of the MWB model (García-Segura 1997, García-Segura et al. 1999) have been quite successful at producing collimated pPNe and PN flows where jets form within the hot bubble far from the star. Magnetic pressure then drives a linear expansion of the jet away from and back toward the star. Such a magnetic spring effect may give velocity segregation seen in some pPNe and PNe. These simulations give very encouraging results in terms of reproducing both morphologies and aspects of the kinematics.

The exact nature of these jets has yet to be explicitly studied. Their formation may be similar to plasma gun effects (Contopoulos 1995). Gardiner & Frank (T.A. Gardiner, A. Frank, unpublished manuscript) recently studied MWBB jets, concluding their formation occurs as axial currents in the hot bubble attempt to achieve cylindrical equilibrium, i.e.,

$$q\frac{1}{\varpi}\frac{d\varpi B_\phi}{d\varpi} = \frac{4\pi}{c} j(\varpi). \tag{7}$$

Here ϖ is the cylindrical radius and j is the axial current. Gardiner & Frank (2001) proposed that flow in the hot bubble can be described as a jet with a non-zero current density in its core surrounded by a current free region where the field has relaxed to a force-free configuration with $B_\phi \propto 1/\varpi$ (Matzner & McKee 1999).

The consensus in other fields however holds that jets are launched and collimated via magnetized accretion disks (Konigl & Pudritz 2000). As discussed before, in their papers on jets in pPNe/PNe, Morris (1987) and Soker & Livio (1994) proposed theoretical models not of the jets themselves but of the formation of accretion disks via binary interactions. The assumption, based on the success of disk-based magneto-centrifugal models in other contexts, was that disks equal jets. Livio (2000, 2001) has extended this conclusion, articulating the view that all jet-bearing systems (YSOs, AGN, microquasars) require both accretion disks and an additional source of energy (Ogilvie & Livio 1998). In the case of PNe, the extra energy may be associated with the luminosity of the central star (Livio 2000). Whereas the models of Blackman et al. (2001a,b) provide more explicit arguments for magneto-centrifugally driven jets in pPNe/PNe, detailed calculations of jet structures and properties must still be carried out. Of course, any model

requiring accretion disks in PNe will likely require a binary companion to act as a mass reservoir (Soker & Rapport 2001, Soker 2001).

BIPOLAR ROTATING EMISSION LINE JETS (BRETS) The objects known as BRETS (López 1997, Guerrero 2000) provide intriguing problems for evolved-star theorists. The immediate interpretation of BRETS as precessing jets has been strengthened by numerical simulations (Cliffe et al. 1995).

It appears difficult to reconcile point symmetry with hydrodynamic collimation mechanisms due to problems of getting the entire torus to precess rigidly on the correct timescales (Frank 1999, Guerrero 2000). García-Segura (1997) demonstrated that precession of stellar magnetic axes (driven by a binary) can produce point symmetric morphologies. García-Segura & López (2001) extended the idea to multipolar nebula via slow axial precession; however, no physical justification for such a configuration was given. A binary companion may also be required for precession in the Blackman et al. (2001) models where only a rapidly rotating star drives the outflows.

The precession of an accretion disk offers a natural means for inducing precession in magneto-centrifugal jet models. Pringle (1996) demonstrated that radiation shadowing from the central star can drive a warping instability in disks surrounding luminous objects. In Livio & Pringle (1996, 1997), these models were applied to PNe where it was shown that the disk precession timescale is comparable to the observed jet precession periods.

ANASE AND FLIERS The nature of bright knots seen along the axis on many elliptical and bipolar PPNe and PNe remains a mystery. Whereas these features may be second-order effects attributable to intrinsically statistical variations in the initial conditions of a particular PN (i.e., "weather" rather than "climate"), the fact that many are oriented along the major axis of the outflows means they might be interpreted as remnants of early phases of outflow collimation.

A number of authors have invoked jets to explain polar FLIERs (Icke 1988, Icke et al. 1992, Frank et al. 1996). These models fare poorly when compared with the many observed morphologies of FLIERs that show bow shocks pointing back toward the central star. Steffen & López (2001) have proposed a stagnation flow model for polar FLIERs. Their scenario employs a time-dependent collimated jet driving into circumstellar material (e.g., the planetary nebulae KjPne 8, Steffen & López 1998). When the jet shuts off, thrust is lost from behind the rapidly cooling plug that forms at the head of the jet. The plug is decelerated as it sweeps up the material ahead of it. This model has promising features because it combines strong collimation and time-dependence in the flow from the star to explain both the presence of short knots and their orientation.

FLIERs and anase have also been modeled as clumps of ambient material subject to photoionization, ablation, and acceleration (the Oort-Spitzer rocket effect). Both analytical and numerical studies of this process have been carried out (Mellema et al. 1998, López-Martín et al. 2001). These models hold some promise

in terms of recovering the kinematics and ionization structures seen in real FLIERs. Unfortunately, they also fail to account for observed morphologies while begging the question of why polar-orientated clumps should exist in the ambient medium to begin with.

Some mix of the jet and photoionized clumps models may be needed to explain FLIERs. Redman & Dyson (1999) have proposed a model in which a clumpy jet experiences mass loading as clump material is ablated and driven downstream. It is noteworthy that the general effect of clumpy flows on PNe (and other astrophysical systems) remains an open one. Dyson, Hartquist, and collaborators have pioneered the study of how clumpy or inhomogeneous flows differ from the smooth flows assumed in the majority of PNe hydro/MHD studies (Dyson et al. 2001). Recent numerical simulations (Poludnenko et al. 2001) and high-energy density laboratory studies (Dannenberg et al. 2001) have also taken up the issue. We agree with Dyson that some fraction of PNe theory may need to be revised in light of clumpy flow dynamics. Thus the issue deserves further theoretical consideration.

Stellar Origins of Disks and Tori

Much of PNe and pPNe shaping theory relies on circumstellar material in either an expanding toroidal density distribution or an accretion disk. Whereas the latter clearly requires a secondary star, it is still not clear if the former can be obtained by a single star. Thus the presence, frequency, and effect of binary companions on PNe evolution remains one of the most contentious issues in the field. Here we briefly review the subject of binary effects (for a review see Iben & Livio 1993, Iben 2000).

SINGLE-STAR MECHANISMS FOR PRODUCING TORI A number models exist for creating circumstellar torii from single stars. All of these mechanisms rely on stellar rotation in some way (Asida & Tuchman 1995) and may require spin-up via a companion. Based on a suggestion by Tom Harrison, Frank (1995), Soker (1998a), and Soker (2000b) have proposed a model where large cool spots on the surface of an AGB star produce increased dust production and an equatorial enhancement of wind density. Dorfi & Höfner (1996) examined the direct coupling of rotation, dust formation, and mass loss, finding that temperature variations in a rapidly spinning AGB star could produce enhanced equatorial mass loss. Matt et al. (2000) found that dipole magnetic fields in an AGB star could guide mass loss along the equator forming a torus. This model clearly requires the presence of a dynamo.

The Wind Compressed Disk (WCD) mechanism of Bjorkman & Cassinelli (1993) has been one of the most promising single-star models explored to date (Owocki et al. 1994). The WCD disk model predicts outflowing excretion disks will form around rapidly rotating stars when streamline are deflected via Coriolis forces. Though the model was originally intended for B[e] stars, it has been applied to other classes of objects including AGB stars (Ignace et al. 1996). In most cases, the rotation rate of the star needs to be a significant fraction of the break-up rate for wind

compression to occur. García-Segura (1997) have noted that the critical rotation rate for break-up depends on the luminosity of the star via

$$\Omega_c = \sqrt{\frac{GM_*(1-\Gamma)}{R_*^3}}, \tag{8}$$

where $\Gamma = L_*/L_{Ed}$ and L_{Ed} is the Eddington luminosity. Ω_c may approach the actual rotation rate of the star as its luminosity increases.

The WCD model links the properties of the stellar progenitor directly to the bipolar bubble producing density and velocity distributions that can be fed directly into hydro or MHD models. Some studies have cast doubt on the effectiveness of the WCD mechanism in line-driven winds (Owocki et al. 1996), and its fate remains a important area of research.

EFFECTS OF BINARY STARS Soker (1997) attempted to distinguish between different classes of binary interaction scenarios affecting PNe shaping. Careful in his use of the term binary because substellar mass companions (brown dwarfs and Jupiter mass planets: Soker 1994b, 1996, 1999; Harpaz & Soker 1994) could also affect shaping, Soker defined nonsingle star evolution as at least one property of the primary being determined by an orbiting object. Soker concluded that the majority of aspherical PNe had undergone a binary interaction. Binaries could be separated into extremely wide binaries with $T_{pn} < T_{orb}$ and $a > 5000$ AU (T_{orb} = orbital period, T_{pn} = PNe lifetime a = orbital separation); wide binaries with $T_{pn} \approx T_{orb}$ and $100 < a < 1000$ AU; close binaries that avoid common envelope phase; or close binaries experiencing common envelope evolution. It is the last two categories that are likely to have the most dramatic effect on PNe evolution. Other promising mechanisms that exist, such as the radiative effects of a secondary on the primary's temperature distribution (Frankowski & Tylenda 2001), deserve further exploration.

Whether close companion(s) ultimately and sufficiently influence the environment to account for the shaping of PNe remains a topic of considerable controversy (Bujarrabal et al. 2000). This is particularly true because both inertial- and self-confinement–based models rely on initial conditions (gaseous torii, magnetic fields) that could be supplied directly from mergers, accretion disks, or tidal torquing resulting from interactions with a binary companion. Thus, regardless of the details of the specific model, binary companions often do something good for nebular shaping (M. Livio, personal communication 2001).

COMMON ENVELOPE (CE) EVOLUTION CE evolution is a consequence of dynamical mass transfer in a close binary system where the more massive star has a deep convective envelope (Rasio & Livio 1996). CE evolution occurs when the more massive, mass-losing star is unable to contract as rapidly as its Roche lobe and envelope material is rapidly transferred to the secondary. The secondary is driven out of thermal equilibrium, and the final configuration is a common envelope shared by both stars, with the cores rotating about the center of mass. Differential rotation

of the binary cores and CE gas leads to energy and angular momentum transfer potentially liberating the entire envelope. Binaries that contain a compact object in a close orbit around the secondary (i.e., whose orbital period is a few days) are thought to have undergone CE evolution. The field has received considerable attention, and a number of excellent reviews on the subject exist (Iben & Livio 1993, Taam & Sandquist 2000).

In the domain of PNe studies, CE evolution has been one of the principal mechanisms believed to produce the expanding slow-wind torus needed in GISW models. One of the principal uncertainties in CE models has been the effectiveness of envelope liberation. The quantity $\alpha_{CE} = \Delta E_{bind}/\Delta E_{orb}$ serves as a measure of CE ejection efficiency. Using a primary mass of $M_p = 5\ \mathrm{M}_\odot$ and and a variety of secondary masses, Livio & Soker (1988) presented results with low values of α_{CE}. More accurate SPH simulations by Rasio & Livio (1996) examined the early phases of CE evolution with a system of similar masses and realistic initial conditions for the primary star. Whereas the simulations tracked only 100 dynamical times of evolution, they did show rapid in-spiral of the secondary and an ejection of approximately 10% of envelope mass. Extrapolating the energy transfer rate, Rasio & Livio concluded that envelope ejection ($\alpha_{CE} = 1$) would occur on timescales of a year. Terman & Taam (1996) also found envelope ejection in systems with extended primaries and more massive companions. Sandquist et al. (1998) followed the later stages of CE evolution of an AGB star with low mass companion. These simulations showed fairly high efficiency of envelope ejection (40%) as the orbit decayed from $P = 200$ days to 1 day. Most importantly, the Sandquist et al. (1998) models showed mass ejection concentrated toward the equatorial plane with $q \approx 5$. The expanding torus had a form similar to those assumed in GISW models. Note that the highest velocities in the ejected material occur near the equator. Thus, the issues raised by Dwarkadas et al. (1996) concerning pole-to-equator velocity contrasts may limit the ability of CE ejection to provide constraining torii.

FORMATION OF ACCRETION DISKS It is unlikely that an accretion disk could survive the long main-sequence lifetime of a PN central star. Thus, accretion disks in PNe systems must form via binary interactions. Disks may form around secondaries via Roche lobe overflow or Bondi accretion of AGB winds (Morris 1981, Morris 1987, Mastrodemos & Morris 1998, 1999). Such systems would be similar to symbiotic stars. Accretion disks could also form around the primary after CE evolution and disruption of the secondary star (Soker & Livio 1994, Miranda 1999). Mastrodemos & Morris (1998), and Soker (1998c) carried out detailed simulations of the first scenario. Using an SPH method they modeled the gravitational interaction of a dense AGB wind with lower mass companion (Figure 4). The models were noteworthy for their inclusion of a host of physical processes including gas-dust interactions in the wind and molecular cooling. Typical parameters for the models were $M_p = 1.5$, $M_s = 1$, and binary separations between 3 and 6 R_p (orbital periods of 4 to 14 years). The orbital separation was close enough for both Roche flow and wind accretion to play a role. Accretion disk formation was seen in all the simulations. The disks were stable throughout the life of the simulations (3–5 orbits or

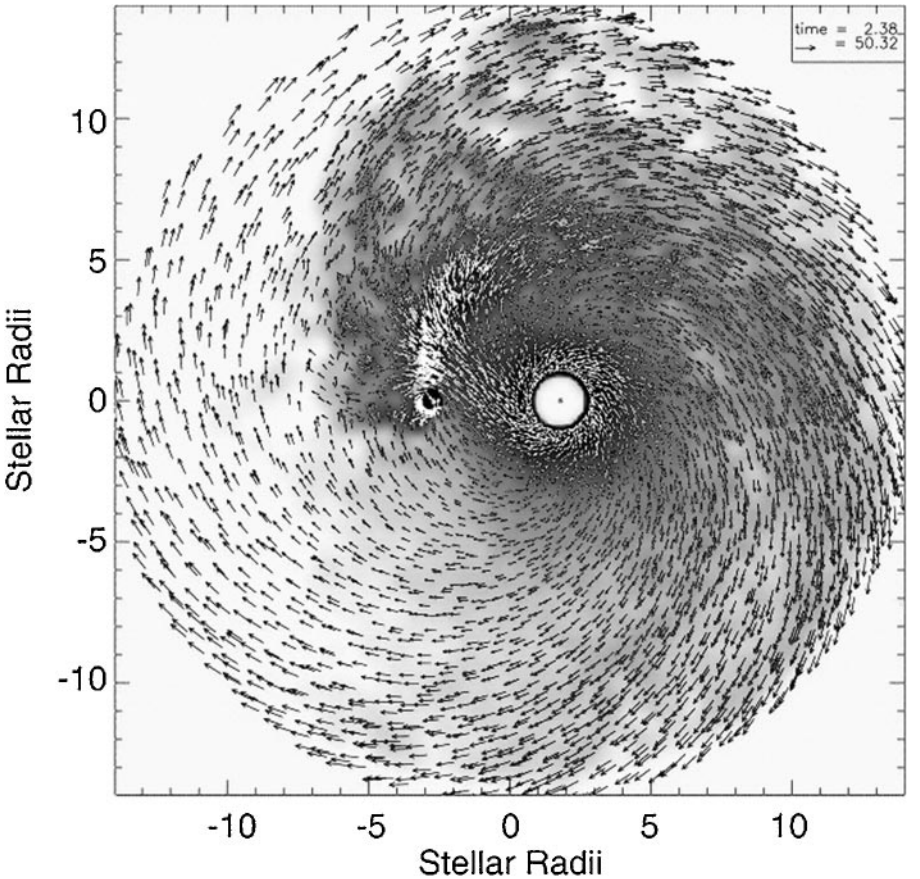

Figure 4 The formation of an accretion disk and a trailing wake associated with a compact companion (*Left*) in a binary system in which the secondary (*Right*) has evolved to an AGB star. The figure shows the results of SPH simulations by Mastrodemos & Morris (1998) in which the density and velocity vector maps of their model M3 are overlaid. The disk and its wake consist of mass accreted from the winds and the Roche-lobe overflows from the AGB star.

>10 accretion flow timescales R_{acc}/v_{acc}) and were geometrically thin owing to strong cooling.

These properties make them amenable to the so-called α disk formalism used in many MHD launching models (Hartmann 1998). The disks also exhibited warping modes that are promising for the development of point-symmetry should jets arise. The size of the disks was shown to vary with the ratio of the orbital to wind speed v_o/v_w. As this ratio increases the secondary becomes more effective at capturing passing wind material. Extrapolations from their models allowed Mastrodemos &

Morris (1998) to set a limiting orbital separation for disk accretion of ≈20 AU. In a second paper, Mastrodemos & Morris (1999) examined a wider range of initial conditions for close binaries that would avoid CE evolution. Beginning with binaries whose companion mass spanned a range 0.25–2 $M_\odot$ and orbital separations of 3.6–50 AU, Mastrodemos & Morris (1999) found a continuous variation in behavior from accretion disk formation through the development of outflowing toroidal density distributions. The latter configurations are of great interest in that density contrasts of $5 < q < 10$ were created. As with the CE models, this is enough to account for shaping via GISW mechanisms. Based on these solutions, they estimated that ≈34% to 40% of all detached binaries will lead to bipolar morphologies.

The formation of accretion disks via disruption of the secondary after CE evolution is an intriguing possibility (Soker & Livio 1994). This model implies a finite lifetime for the disk as the mass reservoir of the distrusted companion is slowly drained onto the primary. Such a mechanism may be attractive in explaining certain transient properties of pPNe outflows (Blackman et al. 2001a). Reyes-Ruiz & López (1999) carried out more detailed calculations disk formation and evolution in this scenario (using α disk models). Their results showed the disk accretion rate decreased as a power-law in time from an initial value of $\dot{M}_a = 10^{-4}$ $M_\odot$/years. The outer disk radius increased with time as a power-law as angular momentum was transferred to outer disk annuli.

CONCLUSIONS AND FUTURE DIRECTIONS

In the early 1990s, confidence was building that interacting winds scenarios might successfully account for the morphologies of PNe. Since 1994 that confidence has been upended by stunning new images from the Hubble Space Telescope, followed shortly thereafter by puzzling results from the Chandra X-ray satellite and various ground-based studies. Simply put, long-standing theories of stellar evolution, mass transfer in binaries, and the effects of putative magnetic fields have been challenged to supply a paradigm in accord with the observations. This challenge has spurred intense research activity in these and related fields which rooted first within the context of mass loss by evolved stars. The outcomes should be applicable to similar outflow phenomena across the H-R diagram, from YSOs and η Carinae to asymmetric supernova detonations and their remnants.

The observational highlights of the past decade are these:

- PNe and their younger neutral counterparts pPNe have complex, fascinating structures that can be systematically classified by common characteristics of their shapes and symmetries.
- Mass loss is isotropic, sometimes percussive and sometimes pulsed on time scales of 1000 years, as stars make their final ascent to the tip of asymptotic giant branch.

- The mode of mass ejection changes in amplitude $\dot{M}$ and symmetry at or shortly after attaining the tip of the AGB, called the post-AGB phase of evolution. Very high-order symmetries are possible, and squid, jellyfish, and starfish shapes are not uncommon.
- Luminous post-AGB stars can eject mass at very high velocities of hundreds of km s^{-1}, up to 100 times in excess of the surface escape velocity and expected surface wind speeds. Additionally, CO observations show that the momentum of the collimated outflows in collimated, high-luminosity pPNe is as much as 1000 times larger than radiatively driven stellar winds can explain.
- The collimation can be extremely effective, with opening angles from a few to tens of degrees not uncommon. In many cases, though not all, the outflows follow a Hubble Flow form in which Doppler shift increases linearly with stellar radius out to the visible end of the nebulosity. Superficially, the ejection of mass seems better described as an event than an ongoing process.
- The onset of ionization in the pPNe-to-PNe transition probably both amplifies and disrupts the complex symmetries owing to the disruptive passage of an ionization front through the nebula. The sudden heating of the gas from 10s to 10,000 degrees probably reshapes and softens the nebular shape.
- Low-ionization knots and jets are found in many highly ionized PNe, generally in pairs, whose nuclear offsets and Doppler speeds are equal and opposite. The speeds of these knots are both highly supersonic and much larger than the material around them, which suggests that the knots and jets were ejected later than the larger, more amorphous gas that surrounds them.
- A direct link between highly collimated outflows and stellar properties has shown that the most collimated PNe are associated with relatively massive ($M > 3\ M_{\odot}$) progenitor stars. However, any direct physical connection between PN morphologies and other nuclear properties that might account for strong flow collimation, e.g., binarity and/or nearby magnetic fields, is weak.

Whereas YSOs have an obvious external reservoir of mass that is rich in angular momentum (and gravitational potential energy) and threaded with magnetic fields upon which to draw, isolated AGB stars do not. The search for an explanation for PN morphologies and kinematics is presently leading in the direction of new ways to look at the evolution of old stars. For example, the formation of bipolar and bilobed PNe requires some sort of fundamentally important axis of symmetry in the ejection system.

One path forward is to assume that external torque from a companion star exerts a substantial influence on the evolution and mass loss of an AGB star, or that mass lost from the AGB star forms an accretion disk on its companion and/or generates a disk from mass overflow. Another is to suppose that AGB stars, particularly the massive ones, harbor deeply hidden magnetized flywheels whose fields once raised to the surface by deep convection, or exposed when the envelope is lost, can define a symmetry axis for the collimated outflows. Although direct observational support for interacting binary systems and magnetic fields is circumstantial at best,

these concepts for accounting for outflow collimation are very popular. pPNe and PNe are ideal laboratories for testing these models owing to their low internal extinctions and high surface brightnesses.

Interacting binary systems were the first of these ideas to receive advocacy by Morris, Livio, Soker, and their many colleagues. They suggest that accretion disks or strong tidal forces from companion stars and/or large planets in orbits near the AGB surface supply large amounts of angular momentum to the highly bloated AGB star with a loosely bound and perhaps pulsationally unstable envelope. Several ingenious mechanisms for generating a disk from this angular momentum have been proposed, including wind streamlines from a star rotating near breakup that converge to the midplane and form a disk; spin-induced levitation and cooling of the equatorial regions forming a torus of dust; and external tidal forces that create a toroidal accretion flow around the entire system. However, whereas disks and tori may be assembled in this way, the high degree of outflow collimation, particularly in high-mass AGB stars, is still difficult to understand. The effects of companion stars stand as fundamental challenges to the community. More work providing explicit links between nebular shapes and specific orbital scenarios will be forthcoming.

As early as 1958 Aller had speculated that magnetic fields played a key dynamical role in the shaping of PNe. Magnetic collimation via weak fields have been applied to PNe by García-Segura, Franco, López, Matt, and their colleagues. Magneto-centrifugal models similar to those used in YSOs have been applied to PNe by Blackman, Frank, and collaborators. Simulations are showing how magnetic fields in rotating and nonrotating environments build disks and, sometimes, collimated polar flows. This work is still in its infancy, the initial results (García-Segura et al. 1999) look very promising (Figure 5), and the outcomes will be of interest to several astrophysics communities. A successful effort requires hard work on both observational and theoretical fronts. The recent detection of milligauss fields embedded in the torus of K3–35 will motivate more work on magnetic collimation processes that are already applicable to other types of collimated astrophysical outflows, including the solar wind. However, the source of sufficiently strong fields to channel the winds of AGB stars is as yet not explained.

Not long ago we believed that the evolution of a planetary nebula could be predicted by one number or perhaps two parameters: progenitor stellar mass and the chemical properties of its ejecta accelerated to winds by surface radiation pressure. If nothing else, the Hubble images warn us that other parameters—perhaps several of them—may need to be added to the prescription for forming PNe. These can include the presence of a companion, the orbital attributes of the companion, the angular momentum of the star at birth, and details of the dredge ups that occur at the tip of the AGB. On top of this, we need to hone our physics of how flows are collimated.

An astrophysically interesting aspect of the study of PNe shaping at this time may be the transition from a single monolithic paradigm (GISW) to a multiplicity of processes whose relative importances will depend on the where, when, and how a star enters its final stages of evolution. A number of authors have noted

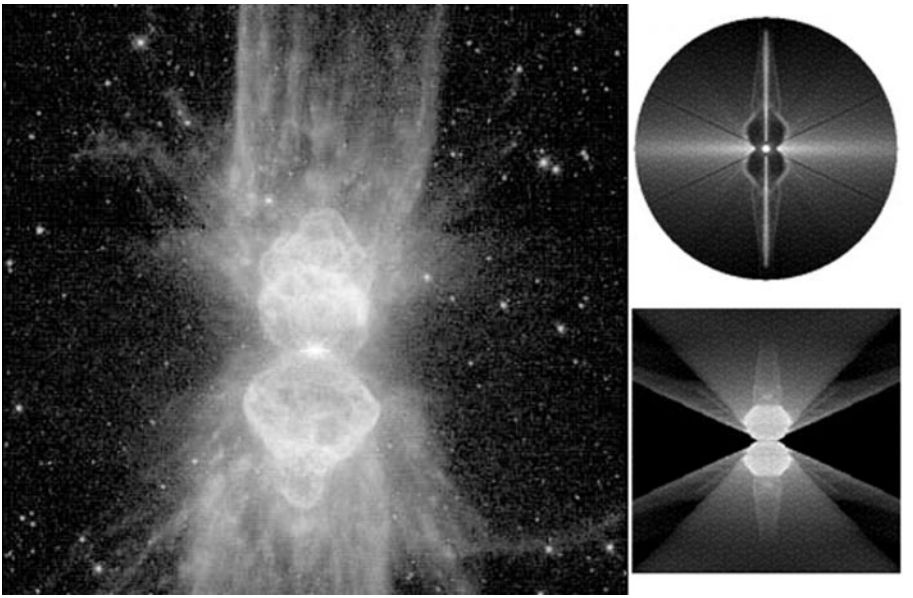

Figure 5 A MWBB Model for the Ant Nebula, Menzel 3. This figure compares an image of Menzel 3, the Ant Nebula (*left*) with results of axisymmetric MHD calculations of the magnetized wind-blown bubble model (*right*, García-Segura et al. 1999). Note the presence of a jet in the two-dimensional density map of the MWBB model (*top right*). Ionization effects produce the filaments seen in the tilted and projected three-dimensional synthetic emission line image (*lower right*).

the similarity of some PNe shapes to the classic images of wave functions for the hydrogen atom. This playful metaphor may provide some inspiration in the coming years. Whereas a new dominant paradigm may emerge, it is also possible that researchers may have to treat the variety of potential shaping processes as a kind set of basis vectors. The projection onto an individual nebula (i.e., which processes actually act on that nebulae) will then have to be read off the object via models that link evolutionary processes to those that yield specific modes of shaping.

Whether we will be led to a new dominant paradigm or a Hilbert space of many coexisting shaping models is unclear. If the past decade has taught us anything, however, ten years from now we can expect, once again, to find ourselves surprised. That's life at the endless frontier.

ACKNOWLEDGMENTS

There are so many people who have contributed to this article that we would have to add many pages to list them all. We are particularly indebted to the following people for the discussions and help: Mario Livio, Eric Blackman, Jack Thomas, Hugh

van Horn, Joel Kastner, Garrelt Mellema, Vincent Icke, Tom Gardiner, Alexei Polundenko. Support to AF was provided at the University of Rochester by NSF grant AST-9702484, NASA grant NAG5-8428, and the Laboratory for Laser Energetics. BB benefitted from the inexhaustible patience of his wife and the serenity and hospitality of the Helen Riaboff Whiteley Center at the Friday Harbor Laboratories of Marine Biology of the University of Washington. AF also wishes to thank his family for their understanding.

The *Annual Review of Astronomy and Astrophysics* is online at http://astro.annualreviews.org

LITERATURE CITED

Abell GO, Goldreich P. 1966. *Publ. Astron. Soc. Pac*. 78:232

Alcolea J, Bujarrabal V, Castro-Carrizo A, Sanchez Contreras C, Neri R, Zweigle J. 2000. See Kastner et al. 2000, p. 347

Alcolea J, Bujarrabal V, Sánchez Contreras C, Neri R, Zweigle J. 2001. *Astron. Astrophys.* 373:932

Aller LH. 1958. *Astron. J.* 63:47

Arthur SJ, Henney WJ, Dyson JE. 1996. *Astron. Astrophys.* 313:897

Asida SM, Tuchman Y. 1995. *Ap. J.* 455:286

Balick B. 1987. *Astron. J.* 94:671

Balick B. 2000. See Kastner et al. 2000, p. 41

Balick B, Alexander J, Hajian AR, Terzian Y, Perinotto M, Patriarchi P. 1998. *Astron. J.* 116:360

Balick B, Perinotto M, Maccioni A, Terzian Y, Hajian A. 1994. *Ap. J.* 424:800

Balick B, Preston HL, Icke V. 1987. *Astron. J.* 94:1641

Balick B, Wilson J, Hajian AR. 2001. *Astron. J.* 121:354

Barnbaum C, Morris M, Kahane C. 1995. *Ap. J.* 450:862

Bjorkman J, Cassinelli J. 1993. *Ap. J.* 409:429

Blackman EG, Frank A, Welch C. 2001a. *Ap. J.* 546:288

Blackman EG, Frank A, Markiel JA, Thomas JH, Van Horn HM. 2001b. *Nature* 409: 485

Bond HE. 2000. See Kastner et al. 2000, p. 115

Borkowski KJ, Blondin JM, Harrington JP. 1997. *Ap. J. Lett.* 482:L97

Borkowski KJ, Harrington JP. 2001. *Ap. J.* 550: 778

Breitschwerdt D, Kahn FD. 1990. *MNRAS* 244: 521

Bryce M, Balick B, Meaburn J. 1994. *MNRAS* 266:721

Bryce M, Meaburn J, Walsh JR. 1992a. *MNRAS* 259:629

Bryce M, Meaburn J, Walsh JR, Clegg RES. 1992b. *MNRAS* 254:477

Bujarrabal V, Castro-Carrizo A, Alcolea J, Sánchez Contreras C. 2001. *Astron. Astrophys.* 377:868

Bujarrabal V, García-Segura G, Morris M, Soker N, Terzian Y. 2000. See Kastner et al. 2000, p. 201

Burrows CJ, Krist J, Hester JJ, Sahai R, Trauger JT, et al. 1995. *Ap. J.* 452:680

Calvet N, Peimbert M. 1983. *Rev. Mex. Astron. Astrofis.* 5:319

Cantó J, Tenorio-Tagle G, Różyczka M. 1988. *Astron. Astrophys.* 192:227

Castro-Carrizo A, Lucas R, Bujarrabal V, Colomer F, Alcolea J. 2001. *Astron. Astrophys.* 368:L34

Cerruti-Sola M, Perinotto M. 1989. *Ap. J.* 345:339

Chevalier RA, Luo D. 1994. *Ap. J.* 435:815

Choudhuri AR. 1998. *The Physics of Fluids and Plasmas: An Introduction for Astrophysicists*, p. 359. New York: Cambridge Univ. Press

Chu Y, Guerrero M, Gruendl RA, Williams RM, Kaler JB. 2001a. *Ap. J. Lett.* 553:L69

Chu Y, Guerrero M, Gruendl RA, Williams RM, Kaler JB. 2001b. *Ap. J. Lett.* 554: L233
Cliffe JA, Frank A, Livio M, Jones J. 1995. *Ap. J. Lett.* 44:L49
Cohen M. 1981. *Publ. Astron. Soc. Pac.* 93:288
Collins TJB, Frank A, Bjorkman JE, Livio M. 1999. *Ap. J.* 512:322
Contopoulos J. 1995. *Ap. J.* 450:616
Corradi RLM, Livio M, Balick B, Munari U, Schwarz HE. 2001. *Ap. J.* 553:211
Corradi RLM, Schwarz HE. 1993a. *Astron. Astrophys.* 269:462
Corradi RLM, Schwarz HE. 1993b. *Astron. Astrophys.* 278:247
Corradi RLM, Schwarz HE. 1995. *Astron. Astrophys.* 293:87
Cox P, Lucas R, Huggins PJ, Forveille T, Bachiller R, et al. 2000. *Astron. Astrophys.* 35:L25
Dannenberg KK, Drake RP, Furnish MD, Knudson JD, Asay JR, et al. 2001. *Bull. Am. Astron. Soc.* 198:6402
Delamarter G. 2000. *The hydrodynamic shaping of planetary nebulae and young stellar objects.* PhD thesis. Univ. Rochester. 224 pp.
Deutsch AJ. 1956. *Ap. J.* 123:210
Dorfi EA, Hoefner S. 1996. *Astron. Astrophys.* 313:605
Doyle S, Balick B, Corradi RLM, Schwarz HE. 2000. *Astron. J.* 119:1339
Dwarkadas VV, Balick B. 1998. *Ap. J.* 497: 267
Dwarkadas VV, Chevalier RA, Blondin JM. 1996. *Ap. J.* 457:773
Dyson JE. 1977. *Ap. Space Sci.* 51:197
Dyson JE, de Vries J. 1972. *Astron. Astrophys.* 20:223
Dyson JE, Williams DA. 1980. *The Physics of the Interstellar Medium.* New York: Halsted
Dyson JE, Hartquist TW, Redman MP, Williams RJR. 2000. *Ap. Space Sci.* 272:197
Frank A. 1994. *Astron. J.* 107:261
Frank A. 1995. *Astron. J.* 110:2457
Frank A. 1999. *New Astron. Rev.* 43:31
Frank A. 2000. See Kastner et al. 2000, p. 225
Frank A, Balick B, Icke V, Mellema G. 1993. *Ap. J. Lett.* 404:L25
Frank A, Balick B, Livio M. 1996. *Ap. J. Lett.* 471:L53
Frank A, Balick B, Riley J. 1990. *Astron. J.* 100:1903
Frank A, Mellema G. 1994a. *Astron. Astrophys.* 289:937
Frank A, Mellema G. 1994b. *Ap. J.* 430:800
Frank A, Mellema G. 1996. *Ap. J.* 472:684
Frankowski A, Tylenda R. 2001. *Astron. Astrophys.* 367:513
García-Segura G. 1997. *Ap. J. Lett.* 489:L189
García-Segura G, Langer N, Różyczka M, Franco J. 1999. *Ap. J.* 517:767
García-Segura G, López JA. 2000. *Ap. J.* 544: 336
García-Segura G, López JA, Franco J. 2001. *Ap. J.* 560:928
Gardiner TA, Frank A. 2001. *Ap. J.* 557:250
Giuliani JL. 1982. *Ap. J.* 256:624
Gómez Y, Rodríguez LF. 2001. *Ap. J. Lett.* 557:L109
Gonçalves DR, Corradi RLM, Mampaso A. 2001. *Ap. J.* 547:302
Guerrero MA. 2000. See Kastner et al. 2000, p. 371
Guerrero MA, Chut Y-H, Gruendl RA, Williams RM, Kaler JB. 2001. *Ap. J. Lett.* 553: L55
Guerrero MA, Manchado A. 1998. *Ap. J.* 508: 262
Guerrero MA, Miranda LF, Chu Y-H, Rodríguez M, Williams RM. 2001. *Ap. J.* 563: 883
Guerrero MA, Villaver E, Manchado A. 1998. *Ap. J.* 507:889
Gurzadyan GA. 1997. *The Physics and Dynamics of Planetary Nebulae.* Berlin/Heidelberg/ New York: Springer-Verlag
Hajian AR, Frank A, Balick B, Terzian Y. 1997. *Ap. J.* 477:22
Han Z, Podsiadlowski P, Eggleton PP. 1995. *MNRAS* 272:800
Harpaz A, Soker N. 1994. *MNRAS* 270:734
Harrington JP, Borkowski KJ. 1994. *Bull. Am. Astron. Soc.* 26:1469
Hartmann L. 1998. *Accretion Processes in Star Formation.* Cambridge, UK/New York: Cambridge Univ. Press

Heger A, Langer N. 1998. *Astron. Astrophys.* 334:210
Henney WJ, Dyson JE. 1992. *Astron. Astrophys.* 261:301
Hrivnak BJ, Kwok S, Su KYL. 1999. *Ap. J.* 524:849
Hrivnak BJ, Kwok S, Su KYL. 2001. *Astron. J.* 121:2775
Hrivnak BJ, Langill PP, Su KYL, Kwok S. 1999. *Ap. J.* 513:421
Huggins PJ, Forveille T, Bachiller R, Cox P. 2000. *Ap. J.* 544:889
Huggins PJ, Healy AP. 1989. *Ap. J.* 346:201
Iben IJ, Livio M. 1993. *Ap. J. Lett.* 406: L15
Iben IJ. 2000. See Kastner et al. 2000, p. 107
Icke V. 1988. *Astron. Astrophys.* 202:177
Icke V, Balick B, Frank A. 1992. *Astron. Astrophys.* 253:224
Icke V, Mellema G, Balick B, Eulderink F, Frank A. 1992. *Nature* 355:524
Icke V, Preston HL, Balick B. 1989. *Astron. J.* 97:462
Ignace R, Cassinelli JP, Bjorkman JE. 1996. *Ap. J.* 459:671
Jura M. 1999. In *IAU Symp. 191: Asymptotic Giant Branch Stars*, ed. T Le Bertr, A Lebre, C Waelkens, p. 603. Dordrecht: Kluwer Acad.
Jura M, Chen C, Werner MW. 2000. *Ap. J.* 541:264
Jura M, Chen C, Werner MW. 2000. *Ap. J. Lett.* 544:L141
Jura M, Kahane C. 1999. *Ap. J.* 521:302
Kahane C, Audinos P, Barnbaum C, Morris M. 1996. *Astron. Astrophys.* 314:871
Kahn FD. 1983. In *IAU Symp. 103: Planetary Nebulae*, ed. DR Flower, p. 305. Dordrecht: Reidel
Kahn FD, Breitschwerdt D. 1990. *MNRAS* 242:505
Kahn FD, Breitschwerdt D. 1990. *MNRAS* 242:209
Kahn FD, West KA. 1985. *MNRAS* 212:837
Kastner JH, Soker N, Rappaport S, eds. 2000. *Asymmetrical Planetary Nebulae II, ASP Conf. Ser. Vol. 199*, San Francisco: Publ. Astron. Soc. Pac.
Kastner JH, Gatley I, Merrill K, Probst R, Weintraub D. 1994. *Ap. J.* 421:600
Kastner JH, Weintraub D, Gatley I, Merrill K, Probst R. 1996. *Ap. J.* 462:777
Kastner JH, Soker N, Vrtilek SD, Dgani R. 2000. *Ap. J. Lett.* 545:L57
Kastner JH, Vrtilek SD, Soker N. 2001. *Ap. J. Lett.* 550:L189
Knapp GR. 1986. *Ap. J.* 311:731
Knapp GR, Jorissen A, Young K. 1997. *Astron. Astrophys.* 326:318
Konigl A, Pudritz RE. 2000. In *Protostars and Planets IV*, ed. V Manning, AP Boss, SS Russell, p. 759. Tucson: Univ. Ariz. Press
Koo BC, McKee CF. 1992. *Ap. J.* 388:93
Kwok S. 1993. See Weinberger & Acker 1993, p. 263
Kwok S. 2000. See Kastner et al. 2000, p. 33
Kwok S, Hrivnak BJ, Su KYL. 2000. *Ap. J. Lett.* 544:L149
Kwok S, Hrivnak BJ, Zhang CY, Langill PL. 1996. *Ap. J.* 472:287
Kwok S, Purton CR, Fitzgerald PM. 1978. *Ap. J. Lett.* 219:L125
Kwok S, Su KYL, Hrivnak BJ. 1998. *Ap. J. Lett.* 501:L11
Lada CJ. 1985. *Annu. Rev. Astron. Astrophys.* 23:267
Lamers HJGLM, Cassinelli JP. 1999. *Introduction to Stellar Winds.* Cambridge, UK: Cambridge Univ. Press
Lebedev SV, Chittenden JP, Beg FN, Bland SN, Ciard A, et al. 2002. *Ap. J.* 564:113
Lery T, Heyvaerts J, Appl S, Norman CA. 1998. *Astron. Astrophys.* 337:603
Lery T, Heyvaerts J, Appl S, Norman CA. 1999. *Astron. Astrophys.* 347:1055
Lindqvist M, Olofsso H, Lucas R, Schöier FL, Neri R, et al. 1999. *Astron. Astrophys.* 351:L1
Livio M. 2000. See Kastner et al. 2000, p. 243
Livio M. 2001. In *Probing the Physics of Active Galactic Nuclei, ASP Conf. Ser.* ed. BM Peterson, RW Pogge, RS Polidan, 224:225. San Francisco: Publ. Astron. Soc. Pac.
Livio M, Pringle JE. 1996. *Ap. J. Lett.* 465:L55
Livio M, Pringle JE. 1997. *Ap. J.* 486:835
Livio M, Soker N. 1988. *Ap. J.* 329:764
Livio M, Soker N. 2001. *Ap. J.* 552:685

López JA. 1997. See Habing & Lamers 1997, p. 180
López JA. 2000. *Rev. Mex. Astron. Astrofis. Conf. Ser.* 9:201
López JA, Meaburn J, Rodríguez LF, Vázque R, Steffen W, Bryce M. 2000. *Ap. J.* 538:233
López JA, Roth M, Tapi M. 1993. *Rev. Mex. Astron. Astrofis.* 26:110
López-Martín L, Raga AC, Mellema G, Henney WJ, Cantó J. 2001. *Ap. J.* 548:288
Lynden-Bell D. 1996. *MNRAS* 279:389
Manchado A, Stanghellini L, Guerrero MA. 1996. *Ap. J. Lett.* 466:L95
Marten H, Szczerba R. 1997. *Astron. Astrophys.* 325:1132
Mastrodemos N, Morris M. 1998. *Ap. J.* 497: 303
Mastrodemos N, Morris M. 1999. *Ap. J.* 523: 357
Matt S, Balick B, Winglee R, Goodson A. 2000. *Ap. J.* 545:965
Matzner CD, McKee CF. 1999. *Ap. J. Lett.* 526:L109
Mauron N, Huggins PJ. 1999. *Astron. Astrophys.* 349:203
Mauron N, Huggins PJ. 2000. *Astron. Astrophys.* 359:707
Meaburn J, Clayton CA, Bryce M, Walsh JR, Holloway AJ, Steffen W. 1998. *MNRAS* 294:201
Meaburn J, Walsh JR. 1989. *Astron. Astrophys.* 223:277
Meixner M. 2000. See Kastner et al. 2000, p. 135
Meixner M, Skinner CJ, Graham JR, Keto E, Jernigan JG, Arens JF. 1997. *Ap. J.* 482:897
Meixner M, Ueta T, Dayal A, Hora JL, Fazio G, et al. 1999. *Ap. J. Suppl.* 122:221
Mellema G, Eulderink F, Icke V. 1991. *Astron. Astrophys.* 252:718
Mellema G. 1994. *Astron. Astrophys.* 290:915
Mellema G. 1995. *MNRAS* 277:173
Mellema G. 1997. *Astron. Astrophys.* 321:L29
Mellema G, Eulderink F, Icke V. 1991. *Astron. Astrophys.* 252:718
Mellema G, Frank A. 1995. *MNRAS* 273:401
Mellema G, Frank A. 1997. *MNRAS* 292:795.
Mellema G, Raga AC, Canto J, Lundqvist P, Balick B, et al. 1998. *Astron. Astrophys.* 331:335
Miranda LF, Gómez Y, Anglada G, Torrelles JM. 2001a. *Nature* 414:284
Miranda LF, Torrelles J, Guerrero M, Vázquez R, Gómez Y. 2001b. *MNRAS* 321:487
Miranda LF, Vázquez R, Corradi RLM, Guerrero M, López JA, Torrelles J. 1999. *Ap. J.* 520:714
Morris M. 1981. *Ap. J.* 249:572
Morris M. 1987. *Publ. Astron. Soc. Pac.* 99: 1115
Morse JA, Davidson K, Bally J, Ebbets D, Balick B, Frank A. 1998. *Astron. J.* 116:2443
Muthu C, Anandarao BG. 2001. *Astron. J.* 121:2106
O'Connor JA, Redman MP, Holloway AJ, Bryce M, López JA, Meaburn J. 2000. *Ap. J.* 531:336
O'Dell CR, Henney WJ, Burkert A. 2000. *Astron. J.* 119:2910
O'dell CR, Ball ME. 1985. *Ap. J.* 289:526.
O'Dell CR, Handron KD. 1996. *Astron. J.* 111:1630
Ogilvie GI, Livio M. 1998. *Ap. J.* 499:329
Olofsson H, Bergman P, Lucas R, Eriksson K, Gustafsson B, Bieging JH. 2000. *Astron. Astrophys.* 353:583
Owocki S, Cranmer S, Blondin J. 1994. *Ap. J.* 424:887
Owocki S, Cranmer S, Gayley KG. 1996. *Ap. J.* 472:L115
Palen S, Fix JD. 2000. *Ap. J.* 531:391
Pascoli G. 1985. *Astron. Astrophys.* 147:257
Pascoli G. 1992. *Publ. Astron. Soc. Pac.* 104: 350
Pascoli G. 1997. *Ap. J.* 489:946
Patriarchi P, Perinotto M. 1991. *Astron. Astrophys. Suppl.* 91:325
Pijpers FP, Habing HJ. 1989. *Astron. Astrophys.* 215:334
Pijpers FP, Hearn AG. 1989. *Astron. Astrophys.* 209, 198
Poludnenko A, Frank A, Blackman E. 2001. *Ap. J.* In press
Priest ER. 1984. *Solar Magnetohydrodynamics, Geophys. Astrophys. Monogr.* Dordrecht: Reidel

Pringle JE. 1996. *MNRAS* 281:357
Rasio FA, Livio M. 1996. *Ap. J.* 471:366
Redman MP, Dyson JE. 1999. *MNRAS* 302:L17
Redman MP, O'Connor JA, Holloway AJ, Bryce M, Meaburn J. 2000. *MNRAS* 312:L23
Reed DS, Balick B, Hajian AR, Klayton TL, Giovanardi S. 1999. *Astron. J.* 118:2430
Reipurth B. 1987. *Nature* 325:787
Reipurth B, Bally J. 2001. *Annu. Rev. Astron. Astrophys.* 39:403
Remington BA, Arnett D, Drake RP, Takabe H. 1999. *Science* 284:1488
Reyes-Ruiz M, López JA. 1999. *Ap. J.* 524:952
Riera A, Balick B, Mellema G, Xilouri K, Terzian Y. 2000. See Kastner et al. 2000, p. 297
Riera A, Garcia-Lario P, Manchado A, Pottasch SR, Raga AC. 1995. *Astron. Astrophys.* 302:137
Różyczka M, Franco J. 1996. *Ap. J. Lett.* 469:L127
Sabbadin F. 1984. *Astron. Astrophys. Suppl.* 58: 273
Sabbadin F, Bianchini A, Hamzaoglu E. 1984. *Astron. Astrophys.* 136:200
Sabbadin F, Bianchini A, Strafella F. 1986. *Astron. Astrophys. Suppl.* 65:259
Sahai R. 1999. *Ap. J. Lett.* 524:L125
Sahai R. 2000. *Ap. J. Lett.* 537:L43
Sahai R, Bujarrabal V, Castro-Carrizo A, Zijlstra A. 2000. *Astron. Astrophys.* 360:L9
Sahai R, Bujarrabal V, Zijlstra A. 1999a. *Ap. J. Lett.* 518:L115
Sahai R, Dayal A, Watson AM, Trauger JT, Stapelfeldt KR, et al. 1999b. *Astron. J.* 118: 468
Sahai R, Nyman L. 2000. *Ap. J. Lett.* 538:L145
Sahai R, Trauger JT. 1998. *Astron. J.* 116:1357
Sahai R, Trauger JT, Watson AM, Stapelfeldt KR, Hester JJ, et al. 1998. *Ap. J.* 493:301
Sahai R, Zijlstra A, Bujarrabal V, Te Lintel Hekkert P. 1999c. *Astron. J.* 117:1408
Sakurai T. 1985. *Astron. Astrophys.* 152:121
Sánchez Contreras C, Bujarrabal V, Miranda LF, Fernández-Figueroa MJ. 2000a. *Astron. Astrophys.* 355:1103
Sánchez Contreras C, Bujarrabal V, Neri R, Alcolea J. 2000b. *Astron. Astrophys.* 357:651
Sánchez Contreras C, Sahai R. 2001. *Ap. J. Lett.* 553:L173
Sandquist EL, Taam RE, Chen X, Bodenheimer P, Burkert A. 1998. *Ap. J.* 500:909
Steffen M, Schönberner D. 2001. In *Post-AGB Objects as a Phase of Stellar Evolution*, ed. R Szczerba, SK Goacuterny, p. 131. Boston/Dordrecht/London: Kluwer
Schwarz HE, Aspin C, Corradi RLM, Reipurth B. 1997. *Astron. Astrophys.* 319:267
Shklovskii I. 1956a. *Astron. Zh.* 33:222
Shklovskii I. 1956b. *Astron. Zh.* 33:315
Simis YJW, Icke V, Dominik C. 2001. *Astron. Astrophys.* 371:205
Skinner CJ, Meixner M, Bobrowsky M. 1998. *MNRAS* 300:L29
Soker N. 1994a. *Astron. J.* 107:276
Soker N. 1994b. *Publ. Astron. Soc. Pac.* 106: 59
Soker N. 1996. *Ap. J.* 468:774
Soker N. 1997. *Ap. J. Suppl.* 112:487
Soker N. 1998a. *Ap. J.* 496:833
Soker N. 1998b. *MNRAS* 299:1242
Soker N. 1998c. In *Cool Stars, Stellar Systems, and the Sun, 10th, ASP Conf. Ser. 154*, ed. RA Donahue, JA Bookbinder, p. 1901. San Francisco: Astron. Soc. Pac.
Soker N. 1999. *MNRAS* 306:806
Soker N. 2000a. *Ap. J.* 540:436
Soker N. 2000b. *MNRAS* 312:217
Soker N. 2001. *Ap. J.* 558:157
Soker N. 2002. *Ap. J.* 568:726
Soker N, Livio M. 1989. *Ap. J.* 339:268
Soker N, Livio M. 1994. *Ap. J.* 421:219
Soker N, Rappaport S. 2001. *Ap. J.* 557:256
Soker N, Zoabi E. 2002. *MNRAS* 329:204
Solf J. 2000. *Astron. Astrophys.* 354:674
Steffen W, López JA. 1998. *Ap. J.* 508:696
Steffen M, Schönberner D. 2000. *Astron. Astrophys.* 357:180
Steffen W, López JA, Lim A. 2001. *Ap. J.* 556:823
Su KYL, Volk K, Kwok S, Hrivnak BJ. 1998. *Ap. J.* 508:744
Taam RE, Sandquist EL. 2000. *Annu. Rev. Astron. Astrophys.* 38:113
Tenorio-Tagle G, Cantó J, Różyczka M. 1988. *Astron. Astrophys.* 202:256

Terman JL, Taam RE. 1996. *Ap. J.* 458:692
Terzian Y, Hajian AR. 2000. See Kastner et al. 2000, p. 33
Trammell SR. 2000. See Kastner et al. 2000, p. 147
Trammell SR, Goodrich RW. 1996. *Ap. J. Lett.* 468:L107
Tsinganos K, Bogovalov S. 2000. *Astron. Astrophys.* 356:989
Ueta T, Fong D, Meixner M. 2001. *Ap. J. Lett.* 557:L117
Ueta T, Meixner M, Bobrowsky M. 2000. *Ap. J.* 528:861
van der Veen WECJ, Habing HJ. 1988. *Astron. Astrophys.* 194:125
van der Veen WECJ, Habing HJ, Geballe TR. 1989. *Astron. Astrophys.* 226:108
Weaver R, McCray R, Castor J, Shapiro P, Moore R. 1977. *Ap. J.* 218:377
Weber EJ, Davis L Jr. 1967. *Ap. J.* 148:217
Weinberger R. 1989. *Astron. Astrophys. Suppl.* 78:301
Weinberger R, Acker A, eds. 1993. *IAU Symp. 155: Planetary Nebulae.* Dordrecht: Kluwer
Willson LA. 2000. *Annu. Rev. Astron. Astrophys.* 38:573
Wood PR. 1997. See Habing & Lamers 1997, p. 297
Wood PR, Alcock C, Allsman RA, Alves D, Axelrod TS, et al. 1999. In *Asymptotic Giant Branch Stars, IAU Symp. 191*, ed. T Le Bertre, A Lebre, C Waelkens, p. 151. Dordrecht: Kluwer
Yorke H, Welz A. 1996. *Astron. Astrophys.* 315:555
Yungelson LR, Tutukov AV, Livio M. 1993. *Ap. J.* 418:794
Zhang CY, Kwok S. 1993. *Ap. J. Suppl.* 88:137
Zuckerman B, Aller LH. 1986. *Ap. J.* 301:772

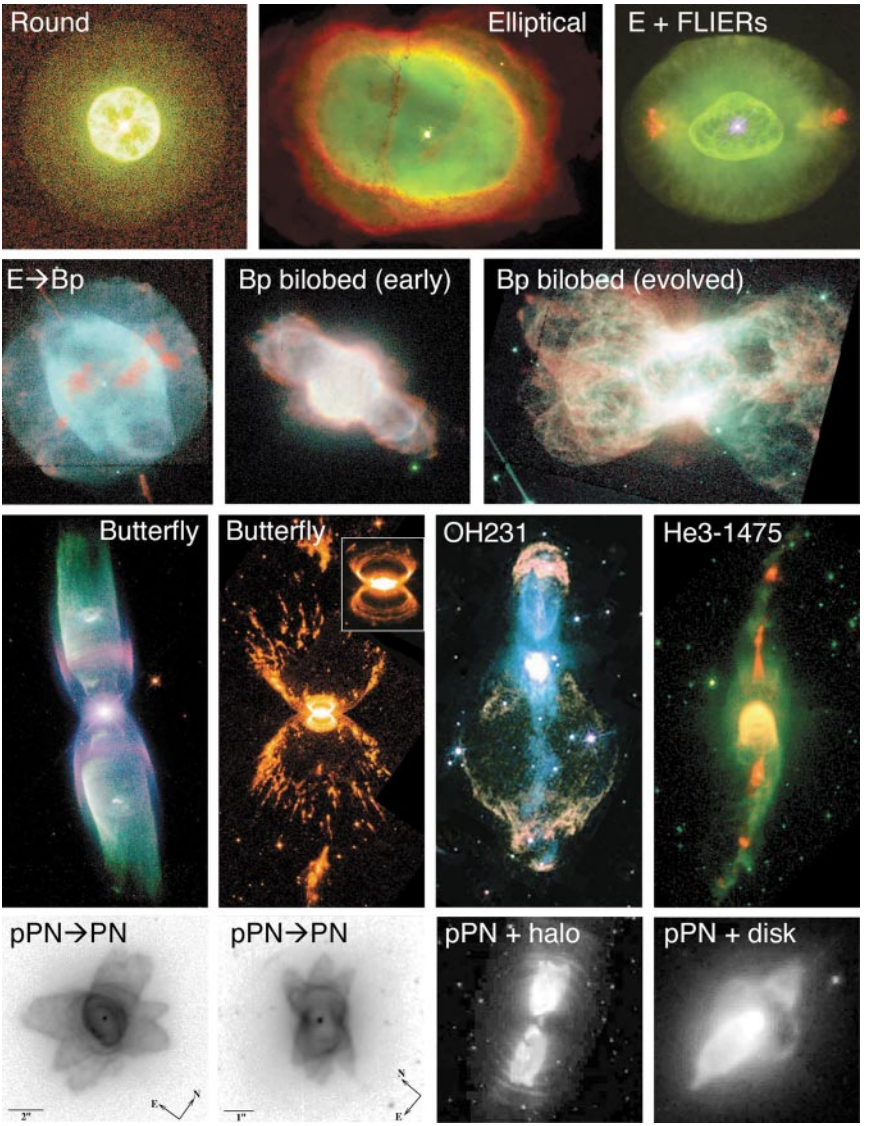

Figure 1 Illustrations of morphological types of PNe and pPNe. Red generally indicates regions of low ionization (colors of NGC 3132 and OH231 have been altered for this purpose). See papers by author for details. (*Top row*) IC 3568 (Bond & NASA), NC 3132 (Sahai & NASA), NC 6826 with FLIERs in red (Balick & NASA); (*Second row*) NC 7354, NC 6886, and NC 7026 (all Hajian & NASA); (*Third row*) M2-9 (Balick & NASA), He2-104 (Corradi & NASA), OH231 (Bujarrabal & ESA), He3-1475 (Borkowski & NASA); (*Bottom row*) He2-47 (Sahai & NASA), He2-339 (Sahai & NASA), IRAS 17150-3224 (Kwok & NASA), IRAS 16594-4656 (Hrivnak & NASA).

Annual Review of Astronomy and Astrophysics
Volume 40, 2002

CONTENTS